An improved tetracycline-inducible expression system for fission yeast

Xiao-Hui Lyu[1], Yu-Sheng Yang[1], Zhao-Qian Pan[1], Shao-Kai Ning[1], Fang Suo[1], Li-Lin Du[1,2,*]

[1]National Institute of Biological Sciences, Beijing 102206, China

[2]Tsinghua Institute of Multidisciplinary Biomedical Research, Tsinghua University, Beijing 102206, China

*Corresponding author: dulilin@nibs.ac.cn (L.-L.D.)

Running head: Inducible system for *S. pombe*.

Keywords: inducible expression system, fission yeast, *Schizosaccharomyces pombe*, tetracycline, conditional loss-of-function

Abstract

The ability to manipulate gene expression is valuable for elucidating gene function. In the fission yeast *Schizosaccharomyces pombe*, the most widely used regulatable expression system is the *nmt1* promoter and its two attenuated variants. However, these promoters have limitations, including a long lag, incompatibility with rich media, and unsuitability for non-dividing cells. Here, we present a tetracycline-inducible system free of these shortcomings. Our system features the *enotetS* promoter, which achieves a similar induced level and a higher induction ratio compared to the *nmt1* promoter, without exhibiting a lag. Additionally, our system includes four weakened *enotetS* variants, offering an expression range similar to the *nmt1* series promoters but with more intermediate levels. To enhance usability, each promoter is combined with a Tet-repressor-expressing cassette in an integration plasmid. Importantly, our system can be used in non-dividing cells, enabling the development of a synchronous meiosis induction method with high spore viability. Moreover, our system allows for the shutdown of gene expression and the generation of conditional loss-of-function mutants. This system provides a versatile and powerful tool for manipulating gene expression in fission yeast.

Summary statement

A new inducible expression system for fission yeast enhances control, offers compatibility with non-dividing cells, and enables synchronous meiosis induction and conditional loss-of-function analysis.

Introduction

Understanding gene function is a central pursuit in biological studies. One important approach to dissecting the function of individual genes is through the artificial manipulation of gene expression levels. Over the past 35 years, a large number of regulatable promoter systems have been developed to enable the manipulation of gene expression in the fission yeast *Schizosaccharomyces pombe*. These systems include glucose-repressible promoters (Hoffman and Winston, 1989; Iacovoni et al., 1999), hormone-inducible promoters (Ohira et al., 2017; Picard et al., 1990), thiamine-repressible promoters and their derivatives (Basi et al., 1993; Garg, 2020; Kjaerulff and Nielsen, 2015; Kumar and Singh, 2006; Maundrell, 1993, 1990; Moreno et al., 2000), tetracycline-inducible promoters (Erler et al., 2006; Faryar and Gatz, 1992; Patterson et al., 2019; Zilio et al., 2012), a copper-repressible promoter (Bellemare et al., 2001), a heat shock-inducible promoter (Fujita et al., 2006), a uracil-inducible promoter (Watson et al., 2011; Watt et al., 2008), an ethanol-inducible promoter (Matsuzawa et al., 2013), and pheromone-inducible promoters (Hennig et al., 2018).

Among the various regulatable promoters available for *S. pombe*, the most popular ones are three thiamine-repressible promoters based on that of the *nmt1* gene (Basi et al., 1993; Maundrell, 1993, 1990). This promoter system offers several advantages. Firstly, the *nmt1* promoter (*Pnmt1*) is a highly active promoter when induced, as *nmt1* ranks as the eighth most highly transcribed protein-coding gene in vegetative cells (340 mRNA molecules per cell) (Marguerat et al., 2012). Secondly, there are two weakened promoter variants, *P41nmt1* and *P81nmt1*, which allow for lower levels of expression, approximately one and two orders of magnitude lower than *Pnmt1*, respectively (Basi et al., 1993). Thirdly, these promoters are strongly repressed in the presence of thiamine, resulting in an around 100-fold difference in expression level between the induced and repressed states (Basi et al., 1993; Vještica et al., 2020). However, this system is not without limitations. It is not compatible with yeast extract-

based rich media that contain thiamine. Additionally, induction requires a medium switch, which incurs time and labor costs. The most significant drawback is that the intracellular thiamine concentration needs to be diluted through several cell doublings before induced expression can occur (Maundrell, 1990; Tommasino and Maundrell, 1991). This results in a long lag time of around 10-12 h and makes the system unsuitable for non-dividing cells such as cells in a quiescent state.

Tetracycline-inducible systems based on the Tet repressor-operator system of the bacterial transposon Tn*10* have been widely used to manipulate gene expression in eukaryotes (Berens and Hillen, 2003; Hillen et al., 1984, 1983). A basic version of the tetracycline-inducible systems consists of three components: the *tet* operator DNA sequence (*tetO*), which is incorporated into a promoter; the Tet repressor protein (TetR), which has a high binding affinity to *tetO*; and a small-molecule inducer that prevents TetR from binding to *tetO*. Commonly used inducers include tetracycline and its analogs anhydrotetracycline (ahTet) and doxycycline. In the absence of the inducer, TetR binds to *tetO* and represses the transcription of the downstream gene. When the inducer is added, TetR no longer binds to *tetO*, and the transcription of the downstream gene is induced.

Three different tetracycline-inducible promoters have been used in fission yeast. In 1992, Faryar and Gatz established the first tetracycline-inducible promoter for fission yeast by incorporating three *tetO* sequences into the cauliflower mosaic virus 35S (CaMV35S) promoter (Faryar and Gatz, 1992). This tetracycline-inducible promoter can be quickly induced, with a reporter protein product becoming detectable within two hours after the addition of an inducer (Faryar and Gatz, 1992). However, an independent study showed that this system has an induction ratio of only 10-fold and the induced expression level is low, similar to that of *P81nmt1* (Forsburg, 1993). In 2012, Zilio et al. adapted a tetracycline-inducible system, originally developed for the budding yeast *Saccharomyces cerevisiae*, for

use in the fission yeast (Bellí et al., 1998; Garí et al., 1997; Zilio et al., 2012). The promoter in this system is composed of seven *tetO* sequences and the basal promoter of the budding yeast *CYC1* gene. The induced level of expression of this promoter is also low, similar to that of *P81nmt1* (Zilio et al., 2012). In 2019, a much stronger tetracycline-inducible promoter, called the *enoTet* promoter (*PenoTet*), was developed by placing three *tetO* sequences into the promoter of the *S. pombe eno101* gene (Patterson et al., 2019). The *eno101* gene is the fourth most highly transcribed protein-coding gene in vegetative cells (470 mRNA molecules per cell) (Marguerat et al., 2012). *PenoTet* achieves an induced expression level about 50% as high as that of *Pnmt1* (Patterson et al., 2019). Unlike the *nmt1* series promoters, these tetracycline-inducible promoters are compatible with rich media, do not need a medium switch for induction, do not exhibit an obvious lag time, and can be used in non-dividing cells. However, these promoters have not been widely adopted, potentially due to the lack of multi-level options, insufficient induced expression levels, non-ideal induction ratios, and the inconvenience associated with the need to introduce both a tetracycline-inducible promoter and a TetR-expressing cassette into a host strain.

In the present study, we have developed an improved tetracycline-inducible expression system for *S. pombe*. This system includes a strong promoter, *PenotetS*, which, similar to *PenoTet*, is derived from the *eno101* promoter but contains only a single *tetO* sequence. *PenotetS* has a high induction ratio of approximately 200-fold and its induced level is similar to that of *Pnmt1*. Additionally, our system includes four weakened variants of *PenotetS*, allowing for five different levels of induced expression. For ease of use, a collection of integration plasmids was constructed, each containing an *enotetS* series promoter and a TetR-expressing cassette. Capitalizing on the compatibility of this system with non-dividing cells, we have developed a new method to induce meiosis, resulting in favorable spore viability and synchrony. Moreover, we have successfully employed this system to generate

110 conditional lethal mutants of essential genes, underscoring its versatility and applicability.

Results

The development of a strong inducible promoter *PenotetS*

It has been shown that in the case of the *GAL1* promoter of *Saccharomyces cerevisiae*, placing a single *tetO* sequence between the TATA box and the transcription start site (TSS) is sufficient to render the promoter strongly repressible by TetR (Murphy et al., 2007). We adopted this approach to modify the 276-bp promoter of the *S. pombe eno101* gene (Wang et al., 2014), which was the basis of the *PenoTet* promoter that contains three *tetO* sequences (Patterson et al., 2019). In *S. pombe* promoters, the TATA box and the TSS, each possessing distinct sequence characteristics, are typically separated by a constant distance (Li et al., 2015; Lu and Lin, 2021; Russell, 1983; Thodberg et al., 2019). To maintain this distance, we substituted a 19-bp sequence between the TATA box and the TSS of the *eno101* promoter with a 19-bp *tetO* sequence (Fig. 1A). We named the modified promoter *PenotetS*, with the letter "*S*" indicating the presence of a single copy of the *tetO* sequence.

A drawback of some of the previously published tetracycline-inducible systems for *S. pombe* is the inconvenience caused by the need to separately introduce a tetracycline-inducible promoter and a TetR-expressing cassette. To establish a user-friendly system, we combined *PenotetS* with a TetR-expressing cassette, which consists of the cytomegalovirus (CMV) promoter and the TetR coding sequence, in a stable integration vector (SIV) (Vještica et al., 2020) (Fig. 1B). The CMV promoter is a robust constitutive promoter in *S. pombe* (Amelina et al., 2016; Toyama and Okayama, 1990). Additionally, downstream of *PenotetS*, we inserted the coding sequence for the yellow fluorescent protein mECitrine, followed by the terminator sequence derived from the *ADH1* gene of *Saccharomyces cerevisiae*. The resulting plasmid was named pDB5318. The fluorescence emitted by mECitrine serves as an indicator of the expression level of *PenotetS*.

In *S. pombe*, previous studies have shown that anhydrotetracycline (ahTet), an analog

136 of tetracycline, is a more effective inducer compared to tetracycline and doxycycline (Erler et
137 al., 2006; Zilio et al., 2012). When an *S. pombe* strain containing pDB5318 was cultured in
138 YES medium supplemented with 2.5 μg/mL of ahTet, a concentration used in a previous
139 study (Zilio et al., 2012), it was observed that the expression level of *PenotetS* was higher
140 than that of the strong constitutive promoter *Padh1* (Fig. 1D). In the absence of ahTet, the
141 expression level of *PenotetS* was markedly lower than that of *Padh1*. Thus, *PenotetS* is an
142 inducible promoter with a high level of induced expression and a substantial induction ratio.
143 To determine whether the expression of TetR or treatment with ahTet affects the growth
144 rate, we conducted a growth curve analysis using a strain containing pDB5318 and a control
145 strain lacking pDB5318 (Fig. S1). The growth rates of both strains were identical in media
146 with or without ahTet, indicating that neither the expression of TetR nor the presence of 2.5
147 μg/mL of ahTet in the culture medium impacted the cell growth rate.
148
149 **The development of four weakened variants of *PenotetS***
150 To provide a range of different expression levels, we developed four weakened variants of
151 *PenotetS*. The design was inspired by a previous study that used GC-rich stem-loop-forming
152 sequences inserted in the 5′ UTR to reduce gene expression (Lamping et al., 2013). It was
153 shown that the extent of expression attenuation increases with the number of GC base pairs
154 in the stem. We selected four different stem-loop-forming sequences used in that study (Fig.
155 1C). Each sequence was inserted immediately downstream of *PenotetS*. The resulting
156 promoters were named *PenotetSW1*, *PenotetSW2*, *PenotetSW3*, and *PenotetSW4*. The
157 letter "*W*" indicates a weakened variant, while the number denotes the expected expression
158 strength, with *PenotetSW1* being the highest and *PenotetSW4* being the lowest.
159 These weakened promoters were combined with the TetR-expressing cassette in an SIV
160 plasmid, following the same procedure as *PenotetS*. In YES medium supplemented with 2.5

161 μg/mL of ahTet, the expression strengths of these promoters varied as expected (Fig. 1D).
162 *PenotetSW1* exhibited an expression level similar to that of *Padh1*, while the other three
163 promoters showed progressively lower levels. In the absence of ahTet, the expression level
164 of each promoter was dramatically lower compared to when ahTet was present, with the
165 three weaker promoters showing fluorescence signals that were indistinguishable from the
166 background.
167
168 **Inducer dose response**
169 We assessed the inducer dose response of *PenotetS* in both YES and EMM media. The
170 inducer ahTet was used at a range of six concentrations (0, 0.004, 0.02, 0.1, 0.5, and 2.5
171 μg/mL). After a 24-hour induction period (which was long enough to reach a steady-state
172 level; see below), the expression levels were measured using the fluorescence signal of the
173 reporter protein mECitrine (Fig. 2). In both types of media, a dramatic transition from a near-
174 minimal level to a near-maximal level was observed between two doses that differed by 5-
175 fold. In YES, this transition occurred between 0.004 μg/mL and 0.02 μg/mL of ahTet (Fig. 2B),
176 while in EMM, it occurred between 0.02 μg/mL and 0.1 μg/mL of ahTet (Fig. 2D). Similar
177 steep dose-response patterns have been observed in other published eukaryotic
178 tetracycline-inducible systems that utilize constitutively expressed TetR as a repressor
179 (Azizoglu et al., 2021; Erler et al., 2006; Nevozhay et al., 2009). We chose to use 2.5 μg/mL
180 of ahTet, an inducer concentration well above the saturating level in both types of media, for
181 subsequent experiments.
182
183 **Induction kinetics in dividing cells**
184 We next assessed the induction kinetics of *PenotetS* and *PenotetSW2* by performing
185 induction time course experiments in both YES and EMM media (Fig. 3). In all time courses,

186 the expression level of the reporter protein mECitrine increased by more than two orders of
187 magnitude within the first 10 hours following the addition of ahTet and ceased to increase
188 after 12 hours. We used the expression level at the 24-hour time point as the steady-state
189 level. In YES medium, for both promoters, at the one-hour time point after adding ahTet to
190 the cultures, the fluorescence signal of mECitrine had already increased by more than one
191 order of magnitude, reaching around 10% of the steady-state level. This rapid increase
192 suggests that both promoters were turned on quickly after the addition of ahTet. In EMM
193 medium, the initial phase of the induction was slightly slower, reaching around 5% of the
194 steady-state level at the one-hour time point. In both types of media, at the four-hour time
195 point, both promoters had reached or surpassed 50% of the steady-state level. By the eight-
196 hour time point, both promoters had reached within 15% of the steady-state level.

197 Upon the activation of an inducible promoter that drives the expression of a protein-
198 coding gene, the level of the protein product reaches a steady state when its synthesis is
199 balanced by its degradation and dilution (Azizoglu et al., 2021; Rosenfeld et al., 2002). The
200 steady-state expression level is determined by both the synthesis rate and the degradation-
201 and-dilution rate, while the induction kinetics are solely determined by the degradation-and-
202 dilution rate (Rosenfeld et al., 2002). Fluorescent proteins are highly stable and have in vivo
203 half-lives longer than 20 hours (Corish and Tyler-Smith, 1999; He et al., 2019; Perruca-
204 Foncillas et al., 2022). In our experimental setup, given that the doubling time of proliferating
205 *S. pombe* cells is around 3 hours (Petersen and Russell, 2016), the degradation-and-dilution
206 rate of mECitrine should mainly be determined by its dilution through cell division. In this
207 scenario, without considering any delay between transcription activation and the formation
208 of mECitrine protein capable of emitting fluorescence, the time required to reach 50% of the
209 steady-state expression level theoretically equals the doubling time (Rosenfeld et al., 2002).
210 However, nascent fluorescent proteins only become fluorescent after undergoing a

211 maturation process, which takes approximately 30 minutes for mECitrine (Azizoglu et al.,
212 2021). Taking this delay into account, the induction kinetics observed in our experiments align
213 closely with immediate or near-immediate transcription activation upon the addition of ahTet.
214 To better characterize the induction kinetics, we performed quantitative modeling by
215 fitting the experimental data to an induction-kinetics model. The resulting fitted curves closely
216 align with our quantitative data, and the half-life parameters derived from the modeling are
217 consistent with our proposed explanation of the expression kinetics (Fig. 3B-D). This analysis
218 further supports the conclusion that transcription activation occurs rapidly upon the addition
219 of ahTet.
220

221 **Quantification of expression levels and comparison with the *nmt1* series promoters**

222 Next, we conducted a comprehensive quantitative analysis of the induced and repressed
223 expression levels of all *enotetS* series promoters in YES and EMM media, and made
224 comparisons with *Padh1* in YES medium and the *nmt1* series promoters in EMM medium
225 (Fig. 4). In YES medium, the induced expression level of *PenotetS* was approximately 1.6-
226 fold that of *Padh1* (Fig. 4A). The fold differences between the induced level of *PenotetS* and
227 the induced levels of the four weakened *enotetS* series promoters were approximately 1.7-
228 fold, 7.1-fold, 30-fold, and 54-fold, respectively (Fig. 4A). The fold differences between the
229 induced and repressed levels (induction ratios) were about 207-fold for *PenotetS* and about
230 226-fold for *PenotetSW1* (Fig. 4A). Since the repressed levels of *PenotetSW2*, *PenotetSW3*,
231 and *PenotetSW4* were very close to the background, we could only determine that these
232 levels were below a threshold (THR) for accurate measurement (Fig. 4A).
233 In EMM medium, the induced and repressed expression levels of the *enotetS* series
234 promoters mirrored those observed in YES medium (Fig. 4B,C). When compared to the *nmt1*
235 series promoters, the induced expression level of *PenotetS* was almost the same as *Pnmt1*

236 and the induced levels of *PenotetSW2* and *PenotetSW4* were similar to those of *Pnmt41* and
237 *P81nmt1*, respectively (Fig. 4B,C). Therefore, in comparison to the *nmt1* series promoters,
238 the *enotetS* series promoters span the same range of induced levels but provide more
239 intermediate levels. Using the mRNA level of the *nmt1* gene in vegetative cells (340 mRNA
240 molecules per cell) as a reference (Marguerat et al., 2012; Rutherford et al., 2024), the
241 induced expression levels of *PenotetS*, *PenotetSW1*, *PenotetSW2*, *PenotetSW3*, and
242 *PenotetSW4* correspond to approximately 365, 219, 57, 13, and 8 mRNA molecules per cell,
243 respectively (Fig. 4D). It is important to note that mRNA levels do not necessarily correlate
244 with protein levels, and the expression of different proteins from the same promoter can result
245 in markedly different protein levels. Regarding repressed expression levels, the *enotetS*
246 series promoters had lower repressed levels than the *nmt1* series promoters when
247 comparing promoters with similar induced levels. In our experiments, *Pnmt1* exhibited only
248 a 26-fold induction ratio, which is lower than the reported induction ratio of around 100-fold
249 (Basi et al., 1993; Vještica et al., 2020). The reason behind this discrepancy is unclear.
250 Nevertheless, even when considering the reported induction ratio for comparison, the
251 *enotetS* series promoters still outperformed the *nmt1* series promoters in this aspect.
252

253 **Induction kinetics and expression levels in quiescent cells**

254 One limitation of the *nmt1* series promoters is their unsuitability for non-dividing cells, as the
255 induction of these promoters requires the dilution of intracellular thiamine through multiple
256 rounds of cell division after shifting the cells to a thiamine-free medium. Tetracycline-inducible
257 systems should be free of this limitation. Therefore, we tested whether *PenotetS* can function
258 in two types of non-dividing cells: cells arrested in the G0 cell cycle phase through nitrogen
259 starvation and spores (Fig. 5).

260 The basal expression levels of *PenotetS* in G0 cells and spores, as reported by the

261 fluorescence of mECitrine, were slightly higher than the basal level in the dividing cells (Fig.
262 5C), presumably due to the lack of dilution of mECitrine through cell division. Upon the
263 addition of ahTet to G0 cells and spores, the expression of mECitrine from *PenotetS*
264 increased several-fold within the first hour and reached a level similar to the steady-state
265 level in the dividing cells at the eight-hour time point. Unlike the situation in the dividing cells,
266 where the expression of mECitrine from *PenotetS* reached a steady state at the 12-hour time
267 point, the level of mECitrine continued to increase in G0 cells and spores after the 12-hour
268 time point (Fig. 5C). The increase did not stop after the 24-hour time point and the level of
269 mECitrine reached several-fold higher than the steady-state level in the dividing cells at the
270 36-hour time point (Fig. 5C). The prolonged rise time and the higher induced levels in G0
271 cells and spores can be explained by the degradation-and-dilution rate of mECitrine no longer
272 being determined by its dilution through cell division but rather by the degradation of
273 mECitrine, which has a long half-life.
274
275 **Meiosis induction in *h+/h+* diploids using *PenotetSW1*-expressed Mc-2A-Mi**
276 In *S. pombe,* the most commonly used method to induce synchronous meiosis is through the
277 inactivation of a negative regulator of meiosis, Pat1, using a temperature-sensitive allele of
278 the *pat1* gene, *pat1-114*, in diploid cells homozygous for the mating type (*h+/h+* or *h−/h−*)
279 (Bähler et al., 1991; Iino and Yamamoto, 1985). However, this approach has several
280 drawbacks, including the use of non-physiological temperature and low spore viability (Bähler
281 et al., 1991; Chikashige et al., 2004; Cipak et al., 2012; Guerra-Moreno et al., 2012;
282 Yamamoto and Hiraoka, 2003). The development of ATP analog-sensitive alleles of *pat1* has
283 enabled the induction of synchronous meiosis at physiological temperature (Cipak et al.,
284 2012; Guerra-Moreno et al., 2012). Moreover, combining Pat1 inactivation with the
285 expression of the *matP*-cassette-encoded protein Pc in *h−/h−* diploids has been shown to

286 elevate spore viability to near-wild-type levels (Cipak et al., 2012; Yamamoto and Hiraoka,
287 2003). Thus, the current state-of-the-art approach for achieving synchronous meiosis with
288 normal spore viability in *S. pombe* requires the combination of two genetic modifications. To
289 showcase the practical utility of our *enotetS* series promoters, we devised a single-plasmid-
290 based method for inducing synchronous meiosis.

291 Diploid *S. pombe* cells that are heterozygous for the mating type (*h+/h−*) can undergo
292 meiosis, whereas those that are homozygous for the mating type (*h+/h+* or *h−/h−*) cannot.
293 This is because the latter lack proteins encoded by one of the two types of mating-type
294 cassettes. In the case of *h+/h+* diploid cells, the missing proteins are the *matM*-cassette-
295 encoded proteins Mc and Mi (Kelly et al., 1988). In our new method for inducing meiosis, we
296 used *PenotetSW1* to induce the expression of Mc and Mi linked by a self-processing 2A
297 peptide (Mc-2A-Mi) in *h+/h+* diploid cells (Fig. 6A). *h+/h+* cells harboring an integration
298 plasmid expressing Mc-2A-Mi under the control of *PenotetSW1* were initially cultured in YES
299 medium and subsequently transferred to EMM−N medium to arrest the cells in G0. Following
300 a 24-hour incubation in EMM−N medium, ahTet was added to induce meiosis. Time course
301 analysis demonstrated the successful induction of synchronous meiosis (Fig. 6B). Tetrad
302 analysis revealed a spore viability of 97% for meiosis induced using this method (Fig. 6C).
303 Thus, we have established a new method for inducing meiosis that is characterized by good
304 synchrony and normal spore viability.

305

306 **Using *enotetS* series promoters to create conditional loss-of-function mutants**

307 Studying the functions of essential genes relies on the creation of conditional loss-of-function
308 mutants. Previously, we developed an auxin-inducible degron (AID) system for generating
309 such mutants in *S. pombe* (Zhang et al., 2022). However, not all genes are compatible with
310 the AID approach. In an unrelated project, we applied the AID method to construct conditional

311 loss-of-function mutants of three essential genes: *ypp1*, *sui1*, and *nrs1*. We first performed
312 endogenous AID tagging in a diploid background and obtained heterozygous tagged diploid
313 strains. Then, we attempted to derive haploid AID-tagged progeny through tetrad dissection
314 (Fig. S2). AID-tagged haploid progeny were readily obtained for *ypp1*. However, no viable
315 AID-tagged haploid progeny were obtained for *sui1* and *nrs1*, possibly due to AID tagging
316 interfering with the function of the protein products of these two genes. We decided to take
317 this opportunity to explore the feasibility of using the *enotetS* series promoters for generating
318 conditional loss-of-function mutants, especially for genes that are not amenable to the AID
319 approach.

320 We first separately deleted *sui1* and *nrs1* in a diploid background to obtain heterozygous
321 deletion diploid strains. Then, for each gene, a plasmid expressing the gene from
322 *PenotetSW2* and a plasmid expressing the gene from *PenotetSW3* were separately
323 integrated into the heterozygous deletion diploid strain. These two promoters were chosen
324 because their induced expression levels are close to the mRNA levels of *sui1* and *nrs1* in
325 vegetative cells (11 and 20 mRNA molecules per cell, respectively) (Marguerat et al., 2012;
326 Rutherford et al., 2024). The resulting strains were subjected to tetrad analysis on YES plates
327 with and without ahTet (Fig. 7). On YES plates without ahTet, for both genes, the basal level
328 expression from neither promoter was able to allow the deletion haploids to form colonies
329 (Fig. 7A). In contrast, on YES plates with ahTet, for both genes, the induced expression from
330 either promoter rescued the inviability of the deletion haploids (Fig. 7A). *PenotetSW2*-driven
331 induced expression in deletion haploids resulted in colony growth indistinguishable from wild
332 type, whereas *PenotetSW3*-driven induced expression resulted in colonies slightly smaller
333 than wild type at 3 days but not at 6 days (Fig. 7A). Thus, we successfully obtained
334 conditional lethal mutants for both genes.

335 To determine how quickly the loss-of-function phenotype arises upon the removal of

336 ahTet, we conducted a growth curve analysis (Fig. 7B). Haploid deletion strains harboring a
337 plasmid expressing the deleted gene from *PenotetSW2* or *PenotetSW3* were pre-cultured in
338 YES liquid medium with ahTet. After the cells were harvested and washed with water, they
339 were transferred to fresh YES medium with and without ahTet. At the six-hour time point, the
340 cultures in the ahTet-free YES medium started to exhibit a noticeably lower growth rate
341 compared to the cultures in the ahTet-containing YES medium. The differences in growth
342 rate became more pronounced as time elapsed. Given that the loss-of-function phenotype
343 does not manifest immediately after the promoter is turned off, but rather arises only after
344 the protein product has been significantly depleted through dilution and degradation, these
345 findings suggest that the *enotetS* series promoters can be rapidly switched off after shifting
346 cells to an ahTet-free medium. Therefore, these promoters provide useful tools for analyzing
347 loss-of-function phenotypes of essential genes in *S. pombe*.

348 **Discussion**

349 In this study, we have developed the *enotetS* series promoters, a new set of tetracycline-
350 inducible promoters for *S. pombe* (Fig. 8). These promoters offer a wide range of expression
351 levels and allow for rapid induction of gene expression in both dividing and non-dividing cells.
352 By combining each of these promoters with a TetR-expressing cassette, this system can be
353 easily implemented in *S. pombe* through a single plasmid transformation. To demonstrate
354 the usefulness of this new inducible expression system, we have successfully developed a
355 new method for inducing synchronous meiosis and generated conditional loss-of-function
356 mutants for two essential genes.

357 Tetracycline and its analogs have traditionally been considered biologically inert to
358 eukaryotic physiology (Gossen et al., 1993). However, recent research has demonstrated
359 that doxycycline, a commonly used inducer in mammalian tetracycline-inducible systems,
360 disturbs mitochondrial protein translation, presumably due to the bacterial origin of
361 mitochondria (Moullan et al., 2015). This raises concerns regarding the use of tetracycline-
362 inducible systems (Chatzispyrou et al., 2015; De Boeck and Verfaillie, 2021; Ohira et al.,
363 2017). Unlike tetracycline and doxycycline, which strongly inhibit bacterial protein translation
364 and belong to the category of “classical tetracyclines”, the inducer used in our system, ahTet,
365 does not effectively inhibit bacterial protein translation and is considered an “atypical
366 tetracycline” (Rasmussen et al., 1991). Therefore, it is unlikely that ahTet negatively affects
367 mitochondrial protein translation. Consistent with this, even though mitochondrial protein
368 translation is essential for *S. pombe* proliferation, studies that have used ahTet on *S. pombe*,
369 including our own, have not observed any detrimental effects on proliferation (Berg and
370 Moseley, 2023; Erler et al., 2006; Lemay et al., 2014; Patterson et al., 2019; Shiroiwa et al.,
371 2011; Sunder et al., 2012; Torres-Garcia et al., 2020; Wang et al., 2018; Zilio et al., 2012).
372 As a precautionary measure against potential unknown side effects of ahTet on *S. pombe*,

373 especially when investigating non-growth phenotypes, we recommend including a strain
374 without an *enotetS* series promoter as a control to rule out the possibility that a phenotype is
375 caused by side effects of ahTet.

376 ahTet is a cost-effective inducer. When used at a concentration of 2.5 μg/mL, the cost of
377 ahTet for making one liter of ahTet-containing medium is about 6 US dollars (based on the
378 list price of Sigma-Aldrich catalog #37919). The ahTet-containing medium should be
379 prepared fresh from the DMSO-dissolved ahTet stock solution before use, as ahTet is not
380 very stable in aqueous solution. It has been reported that ahTet has a half-life of around 30
381 hours in culture media at 30°C (Politi et al., 2014).

382 A higher level of ahTet is required for induction in EMM than in YES (Fig. 2), and the
383 induction kinetics appear to be slightly slower at the early stage of induction in EMM than in
384 YES (Fig. 3). We speculate that these differences may be due to a reduced uptake of ahTet
385 in EMM. It has been reported that the addition of 5 mM of Mg^{2+} to the culture medium
386 diminishes the uptake of tetracycline into *E. coli* cells (Zhang et al., 2014). EMM contains a
387 notably higher concentration of Mg^{2+} (5.2 mM) than YES (less than 0.5 mM) (Li et al., 2020;
388 Petersen and Russell, 2016).

389 The five induced expression levels of the *enotetS* series promoters offer a wide range
390 of possibilities for manipulating gene expression levels. In theory, even more intermediate
391 expression levels can be obtained by titrating the inducer dose. However, the *PenotetS*
392 promoter (and likely its weakened variants) exhibits a steep dose-response curve. This
393 means that the range of inducer doses over which the promoter is responsive, known as the
394 input dynamic range, is narrow. Consequently, precise adjustments to expression levels by
395 altering the inducer dose can be challenging (Azizoglu et al., 2021). If desired, the input
396 dynamic range can be expanded by implementing negative auto-regulation of TetR (Azizoglu
397 et al., 2021; Madar et al., 2011; Nevozhay et al., 2009; Patterson et al., 2019).

398 The use of the *enotetS* series promoters to generate conditional lethal mutants of
399 essential genes is a valuable alternative to the AID method, especially for genes that cannot
400 tolerate AID tagging. This strategy, known as promoter shut-off, has previously been
401 implemented in *S. pombe* using the *nmt1* series promoters and has successfully revealed
402 the loss-of-function phenotypes of many essential genes (Bestul et al., 2021; Kelly et al.,
403 1993; Matynia et al., 2002; Ottilie et al., 1995; Petersen and Hagan, 2003; Tajadura et al.,
404 2004; Wang et al., 2002; Westwood et al., 2004; Win et al., 2004; Yue et al., 2014). Compared
405 to the *nmt1* series promoters, the *enotetS* series promoters offer more levels of expression
406 and larger ratios between induced and repressed conditions. Therefore, they are expected
407 to be better tools for promoter shut-off.
408 While we generated the promoter shut-off strains for *sui1* and *nrs1* by first establishing
409 heterozygous deletion diploid strains and then deriving haploid strains, it should be feasible
410 to directly obtain promoter shut-off haploid strains by inserting an *enotetS* series promoter,
411 along with the TetR-expressing cassette, upstream of the target essential gene using a
412 single-step CRISPR-based marker-free knock-in (Jacobs et al., 2014; Zhang et al., 2018).
413 The intended knock-in clones can be readily selected based on their ability to grow on ahTet-
414 containing plates but not on ahTet-free plates. Promoter shut-off using the *nmt1* series
415 promoters can be initiated by simply adding thiamine to the culture, whereas promoter shut-
416 off using the *enotetS* series promoters requires the more laborious process of washing cells
417 to remove ahTet. It would be worth exploring in the future the feasibility of implementing the
418 method of light-induced inactivation of ahTet for shutting off the *enotetS* series promoters
419 (Baumschlager et al., 2020).
420

421 ## Materials and methods

422 ### Plasmid construction

423 The plasmids used in this study are listed in Table S1, and the primers used in this study are
424 listed in Table S2. We amplified the 276-bp *eno101* promoter (Wang et al., 2014) from
425 genomic DNA using primers oYY1 and oYY2. This amplified promoter was then cloned
426 between the SwaI and XhoI sites in the stable integration vector (SIV) pAV0714 (Addgene
427 plasmid 133479), replacing the *act1* promoter (Vještica et al., 2020). The resulting plasmid
428 was named pDB5530. For the construction of the *enotetS* promoter (*PenotetS*), a 19-bp
429 sequence between the TATA box and the transcription start site (TSS) of the *eno101*
430 promoter in pDB5530 was replaced with a 19-bp *tetO* sequence, specifically that of the O_2
431 operator from the bacterial transposon Tn*10* (TCCCTATCAGTGATAGAGA) (Hillen et al.,
432 1984, 1983; Wray and Reznikoff, 1983). This alteration was accomplished by performing
433 overlapping PCR using pDB5530 as the template and oXH5, oXH6, oXH7, and oXH8 as
434 primers, and then cloning the PCR product between the PacI and HpaI sites in pDB5530.
435 The resulting plasmid was named pDB5531. To use *PenotetS* to drive the expression of the
436 yellow fluorescent protein mECitrine, which serves as a reporter protein, we replaced the
437 *adh1* promoter in pDB4915, a modified SIV plasmid containing mECitrine, with *PenotetS*.
438 pDB4915 was derived from the SIV plasmid pAV0585 (pAde6^{PmeI}-hphMX, Addgene plasmid
439 133472) (Vještica et al., 2020), by altering the linearization site from PmeI to NotI and
440 introducing the *adh1* promoter, the coding sequence of mECitrine, and the terminator of the
441 *Saccharomyces cerevisiae ADH1* gene. *PenotetS* was amplified from pDB5531 using
442 primers oXH17 and oXH18, and then cloned between the ApaI and NheI sites in pDB4915.
443 The resulting plasmid was named pDB5532.

444 To construct an integration plasmid that contains both *PenotetS* and a TetR-expressing
445 cassette, we amplified a TetR expression cassette containing the cytomegalovirus promoter

446 (*P.CMV*) and the coding sequence of TetR from pDM291-tetR-tup11Δ70 (Addgene plasmid
447 41027) (Zilio et al., 2012), using primers oXH19 and oXH47. The amplified cassette was then
448 cloned into the KpnI site in pDB5532. The resulting plasmid was named pDB5318. To
449 construct weakened variants of *PenotetS*, we used primers oXH34-oXH38 to amplify four
450 PCR products, each containing *PenotetS* and a stem-loop-forming sequence immediately
451 downstream of *PenotetS*. These PCR products were then cloned separately between the
452 ApaI and NheI sites in pDB5318, generating four different plasmids, which were named
453 pDB5319-pDB5322. The four weakened variants of *PenotetS* in these four plasmids were
454 named *PenotetSW1*, *PenotetSW2*, *PenotetSW3*, and *PenotetSW4*. The plasmids pDB5318-
455 pDB5322 have been deposited at Addgene (Addgene plasmids 204828-204832) and the
456 Yeast Genetic Resource Center of Japan (YGRC/NBRP) (NBRP IDs FYP6242-6246). The
457 SnapGene files for these plasmids are provided in a compressed folder as a supplementary
458 file.

459 The DNA sequence encoding Mc-2A-Mi was synthesized by BGI Tech Solutions (Beijing
460 Liuhe) and consists of three parts: the coding sequence of Mi, a 60-bp segment encoding
461 the 20-amino acid T2A peptide (RAEGRGSLLTCGDVEENPGP) (Beekwilder et al., 2014),
462 and the coding sequence of Mc. To construct a plasmid expressing Mc-2A-Mi, the Mc-2A-Mi
463 sequence was amplified using primers oXH161 and oXH162, and then cloned between the
464 NheI and BglII sites of pDB5319, replacing the coding sequence of mECitrine. In the resulting
465 plasmid (pDB5533), Mc-2A-Mi is under the control of *PenotetSW1*.

466 The plasmids pDB4877, pDB4878, and pDB4879 were derived from the SIV vector
467 pAV0585 (pAde6^{PmeI}-hphMX, Addgene plasmid 133472) (Vještica et al., 2020), by altering
468 the linearization site from PmeI to NotI and introducing the *nmt1* promoter, the *41nmt1*
469 promoter, or the *81nmt1* promoter, respectively, along with the coding sequence of mECitrine,
470 and the terminator of the *Saccharomyces cerevisiae ADH1* gene. The plasmids pDB5534,

471 pDB5535, pDB5536, pDB5537, and pDB5538 were derived from the SIV plasmid pAV0586
472 (pLys3^{BstZ17I}-bsdMX, Addgene plasmid 133473), by altering the linearization site from
473 BstZ17I to NotI and introducing the TetR expression cassette, an *enotetS* series promoter,
474 the coding sequence of mECitrine, and the terminator of the *Saccharomyces cerevisiae*
475 *ADH1* gene. To construct plasmids expressing *nrs1*, the coding sequence of *nrs1* was
476 amplified from genomic DNA and cloned into pDB5537 and pDB5536, replacing the coding
477 sequence of mECitrine in each plasmid. The resulting plasmids were named pDB5539 and
478 pDB5541, respectively. Two plasmids expressing *sui1* were similarly constructed, except
479 cDNA was used as the amplification template, and they were named pDB5540 and pDB5542.
480

481 **Strain construction**

482 The *S. pombe* strains used in this study are listed in Table S3. Strains containing an
483 integrated plasmid were constructed by linearizing an SIV plasmid with NotI and then
484 transforming the plasmid into a host strain. Correct integration of the plasmid into the *ade6*
485 or *lys3* locus was verified using colony PCR (Vještica et al., 2020). Deletion strains were
486 created using PCR-based gene deletion. Strains with a gene endogenously tagged at the C-
487 terminus with the 3×sAID tag were generated through PCR-based gene tagging (Zhang et
488 al., 2022). The *h+/h−* diploid strain DY51002 was constructed by crossing two haploid strains
489 with *ade6-M210* and *ade6-M216* mutations, respectively. The two haploid strains were pre-
490 grown on YES plates and then mixed in an equal ratio in 20 μL of water. The mixture was
491 spotted on SPA plates with necessary supplements. After approximately 12 hours of
492 incubation at 30°C, cells were collected and plated on YE plates containing 200 mg/L guanine
493 at a density of approximately 10^4 cells per plate. Guanine was used to inhibit the uptake of
494 adenine, thereby preventing the growth of adenine auxotrophs and allowing only the growth
495 of *ade6-M210*/*ade6-M216* diploid cells, which are adenine prototrophs due to interallelic

496 complementation (Cummins and Mitchison, 1967; Smith, 2009). After incubating for 3 days
497 at 30°C, colonies formed on the guanine-containing plates were streaked on YE2A plates. A
498 diploid clone that showed high spore viability in tetrad analysis was saved as DY51002. A
499 prototrophic *h+/h−* diploid strain, DY50999, constructed in the same way as DY51002, was
500 plated on YEPD plates, and colonies that were unable to form spores were selected based
501 on iodine staining. The mating type of the non-sporulating diploid clones was determined by
502 colony PCR, and an *h+/h+* diploid strain was saved as DY51000.
503
504 **Media and growth conditions**
505 The compositions of the media were as described (Petersen and Russell, 2016).
506 Anhydrotetracycline hydrochloride (ahTet; J&K Scientific, catalog number 541642) was
507 dissolved in DMSO at a concentration of 5 mg/mL and stored at −80°C.
508 To analyze the dose response of the inducer, the cells were first cultured in liquid YES
509 medium or EMM medium with the necessary supplements until they reached the logarithmic
510 phase. The DMSO-diluted ahTet stock was then added to achieve the desired concentrations,
511 with an equal volume of DMSO serving as the control. After 24 hours of culturing (with
512 cultures diluted when the OD600 approaching 1.0) at 30°C, logarithmic phase cells were
513 collected for live-cell imaging.
514 For the time course assay of proliferating cells, the cells were first cultured in liquid YES
515 medium or EMM medium with the necessary supplements until they reached the logarithmic
516 phase at 30°C. After adding ahTet to the medium, the cells were collected at specific time
517 points. During the time course, the cultures were diluted when the OD600 approached 1.0.
518 To quantify the expression levels of the *enotetS* series promoters, induced expression
519 levels were measured after transferring logarithmic phase cells to media with 2.5 μg/mL ahTet
520 for 24 hours at 30°C. Repressed expression levels were measured after transfer to media

521 with DMSO under the same conditions.

522 To quantify the expression levels of the *nmt1* series promoters, the cells were first
523 cultured in EMM medium containing thiamine until they reached the logarithmic phase. Then,
524 to measure the induced expression levels, the cells were washed three times with water,
525 transferred to EMM medium without thiamine, and grown at 30°C for 24 hours. To measure
526 the repressed expression levels, the cells were cultured in EMM medium containing thiamine
527 at 30°C for 24 hours.

528 For the time course assay of G0 phase cells, logarithmically growing cells grown in EMM
529 medium were washed three times with water and shifted to EMM medium without nitrogen
530 (EMM−N) for 24 hours at 30°C to arrest the cells in the G0 phase. After adding ahTet to the
531 medium at a concentration of 2.5 μg/mL, the cells were collected at specific time points.

532 For the time course assay of spores, h^{90} cells grown in YES medium were washed three
533 times with water and shifted to MSL−N medium at 30°C for 48 hours to induce sporulation.
534 Then, the cells were collected and treated with Snailase (Beijing Solarbio Science &
535 Technology Co.,Ltd., catalog number S8280) in water at 30°C for 24 hours to digest non-
536 spore cells. After digestion, spores were purified by centrifugation in Percoll solutions. Spores
537 were incubated in EMM−N medium overnight. Then ahTet was added to the EMM−N medium.
538 After adding ahTet to the medium at a concentration of 2.5 μg/mL, spores were collected at
539 specific time points.

540 For the growth curve analysis, haploid deletion strains harboring a plasmid expressing
541 the deleted gene from *PenotetSW2* or *PenotetSW3*, along with a wild-type strain were pre-
542 cultured in YES liquid medium supplemented with ahTet until they reached the logarithmic
543 phase at 30°C. Then, the cells were washed three times with water and transferred to either
544 YES medium or YES medium supplemented with ahTet. The optical density at 600 nm
545 (OD600) of each culture was measured at specific time points, with cultures being diluted if

546 the OD600 approached 1.0. The number of generations was determined based on the
547 OD600 and the dilution ratio.
548
549 **Fluorescence microscopy and image quantification**
550 Live-cell imaging was performed using a Dragonfly 200 spinning disk confocal microscope
551 system (Andor Technology) equipped with an mCherry/YFP/CFP filter set and an
552 mCherry/GFP filter set. Images were acquired with a 100×, 1.4-NA objective using a Sona
553 sCMOS camera and analyzed with Fiji (ImageJ).
554 To quantify the expression level of mECitrine, first, channels of images were split and
555 the DIC channel was used to segment cell boundaries using Cellpose (version 2.1.1)
556 (Stringer et al., 2021). The resulting masked images were processed with the LabelsToRois
557 plugin (Waisman et al., 2021) in Fiji (Schindelin et al., 2012). This plugin generated outlines
558 outlining the boundaries of each cell. Subsequently, the generated outlines were
559 superimposed onto the mECitrine channel. Fiji was employed to calculate the mean
560 fluorescence intensity for each individual cell.
561 In total, three images were acquired for each sample, with each image containing
562 between 50 and 200 cells. The median fluorescence intensity of cells within each image was
563 calculated and averaged across the triplicate images. Background fluorescence was
564 measured using a parental strain that lacked mECitrine and was subsequently subtracted.
565 The resulting fluorescence intensity provided a measurement of the expression level. For all
566 fluorescence quantification results, we conducted two or more biological replicates, each
567 yielding consistent outcomes.
568
569 **Induction and monitoring of meiosis**
570 Log-phase cells grown in YES medium were collected, washed three times with water,

resuspended in EMM medium without nitrogen (EMM−N), and incubated at 30°C for 24 hours to arrest cells in the G0 phase. Then, ahTet was added to the culture at a final concentration of 2.5 μg/mL to induce meiosis. At specific time points, cells were collected and fixed using 70% ethanol. The advancement of meiosis was evaluated by quantifying the number of nuclei per cell after staining the DNA with SYTOX Green (Thermo Fisher, catalog number S7020). For SYTOX Green staining, the fixed cells were washed once with water, resuspended in water containing 1 μM SYTOX Green, and incubated in the dark at room temperature for 5 minutes. The number of nuclei per cell was determined through imaging. The experiment was conducted in three biological replicates, with one replicate presented as representative data in the figure.

Tetrad analysis

To examine spore viability of induced meiosis, cells collected 24 hours after meiosis induction were streaked onto YES plates. Tetrad analysis was carried out using a TDM50 tetrad dissection microscope (Micro Video Instruments, Avon, USA) on YES plates. To assess whether the exogenous expression of *nrs1* or *sui1* can complement the deletion of the corresponding endogenous gene, diploid strains freshly grown on YE2A plates were spotted onto SPASK plates. The SPASK plates were incubated at 30°C for about 24 h. Subsequently, tetrad analysis was carried out on YES plates with and without ahTet.

Curve fitting

The induction kinetics data were fitted using Equation 1, as shown below.

$t \leq lag, y = base,$

$t > lag, y = base + (max - base) * (1 - e\text{^}(-(t - lag) * \frac{ln(2)}{half\text{-}life}))$, (1)

In this equation, "lag" represents the time required for the newly expressed reporter

protein to become detectable, set to 0.5 hours because mECitrine, the reporter protein used, takes approximately 30 minutes to mature and emit fluorescence. "Base" denotes the expression level of the reporter protein at t = 0, set to the quantified value at that time. "Max" indicates the steady-state expression level. "Half-life" refers to the half-life of the reporter protein, determined by both protein degradation and dilution through cell doubling. Curve fitting was performed using the lmfit library in Python, employing the leastsq method (Newville et al., 2016).

Disclosure on the use of artificial intelligence tools

The manuscript was proofread using the artificial intelligence tool editGPT. Following the use of this tool, the authors carefully reviewed and edited the content as necessary. The authors assume full responsibility for the publication's content.

Acknowledgements

We thank the Sophie Martin laboratory for making the SIV plasmids they have developed available through Addgene and the Yeast Genetic Resource Center of Japan (YGRC/NBRP). We thank YGRC/NBRP for providing the plasmids.

Competing interests

No competing interests declared.

Funding

This work was supported by funding from the Ministry of Science and Technology of the People's Republic of China, the Beijing municipal government, and Tsinghua University.

Data and resource availability

Data availability: All relevant data can be found within the article and its supplementary information.

References

Amelina, H., Moiseeva, V., Collopy, L.C., Pearson, S.R., Armstrong, C.A., Tomita, K. (2016). Sequential and counter-selectable cassettes for fission yeast. BMC Biotechnol 16, 76. https://doi.org/10.1186/s12896-016-0307-4

Azizoglu, A., Brent, R., Rudolf, F. (2021). A precisely adjustable, variation-suppressed eukaryotic transcriptional controller to enable genetic discovery. Elife 10, e69549. https://doi.org/10.7554/eLife.69549

Bähler, J., Schuchert, P., Grimm, C., Kohli, J. (1991). Synchronized meiosis and recombination in fission yeast: observations with pat1-114 diploid cells. Curr Genet 19, 445–451. https://doi.org/10.1007/BF00312735

Basi, G., Schmid, E., Maundrell, K. (1993). TATA box mutations in the Schizosaccharomyces pombe nmt1 promoter affect transcription efficiency but not the transcription start point or thiamine repressibility. Gene 123, 131–136. https://doi.org/10.1016/0378-1119(93)90552-E

Baumschlager, A., Rullan, M., Khammash, M. (2020). Exploiting natural chemical photosensitivity of anhydrotetracycline and tetracycline for dynamic and setpoint chemo-optogenetic control. Nat Commun 11, 3834. https://doi.org/10.1038/s41467-020-17677-5

Beekwilder, J., van Rossum, H.M., Koopman, F., Sonntag, F., Buchhaupt, M., Schrader, J., Hall, R.D., Bosch, D., Pronk, J.T., van Maris, A.J.A. et al. (2014). Polycistronic expression of a β-carotene biosynthetic pathway in Saccharomyces cerevisiae coupled to β-ionone production. J Biotechnol 192 Pt B, 383–392. https://doi.org/10.1016/j.jbiotec.2013.12.016

Bellemare, D.R., Sanschagrin, M., Beaudoin, J., Labbé, S. (2001). A novel copper-regulated promoter system for expression of heterologous proteins in Schizosaccharomyces pombe. Gene 273, 191–198. https://doi.org/10.1016/s0378-1119(01)00591-1

Bellí, G., Garí, E., Piedrafita, L., Aldea, M., Herrero, E. (1998). An activator/repressor dual system allows tight tetracycline-regulated gene expression in budding yeast. Nucleic Acids Res 26, 942–947. https://doi.org/10.1093/nar/26.4.942

Berens, C., Hillen, W. (2003). Gene regulation by tetracyclines. Constraints of resistance regulation in bacteria shape TetR for application in eukaryotes. Eur J Biochem 270, 3109–3121. https://doi.org/10.1046/j.1432-1033.2003.03694.x

Berg, R.A., Moseley, J.B. (2023). Regulation of cell size and Wee1 kinase by elevated levels of the cell cycle regulatory protein kinase Cdr2. J Biol Chem 299, 102831. https://doi.org/10.1016/j.jbc.2022.102831

Bestul, A.J., Yu, Z., Unruh, J.R., Jaspersen, S.L. (2021). Redistribution of

661 centrosomal proteins by centromeres and Polo kinase controls partial nuclear envelope
662 breakdown in fission yeast. Mol Biol Cell 32, 1487–1500.
663 https://doi.org/10.1091/mbc.E21-05-0239
664 **Chatzispyrou, I.A., Held, N.M., Mouchiroud, L., Auwerx, J., Houtkooper, R.H.**
665 (2015). Tetracycline antibiotics impair mitochondrial function and its experimental use
666 confounds research. Cancer Res 75, 4446–4449. https://doi.org/10.1158/0008-
667 5472.CAN-15-1626
668 **Chikashige, Y., Kurokawa, R., Haraguchi, T., Hiraoka, Y.** (2004). Meiosis induced
669 by inactivation of Pat1 kinase proceeds with aberrant nuclear positioning of
670 centromeres in the fission yeast Schizosaccharomyces pombe. Genes Cells 9, 671–684.
671 https://doi.org/10.1111/j.1356-9597.2004.00760.x
672 **Cipak, L., Hyppa, R.W., Smith, G.R., Gregan, J.** (2012). ATP analog-sensitive Pat1
673 protein kinase for synchronous fission yeast meiosis at physiological temperature. Cell
674 Cycle 11, 1626–1633. https://doi.org/10.4161/cc.20052
675 **Corish, P., Tyler-Smith, C.** (1999). Attenuation of green fluorescent protein half-life
676 in mammalian cells. Protein Eng 12, 1035–1040.
677 https://doi.org/10.1093/protein/12.12.1035
678 **Cummins, J.E., Mitchison, J.M.** (1967). Adenine uptake and pool formation in the
679 fission yeast Schizosaccharomyces pombe. Biochim Biophys Acta 136, 108–120.
680 https://doi.org/10.1016/0304-4165(67)90326-1
681 **De Boeck, J., Verfaillie, C.** (2021). Doxycycline inducible overexpression systems:
682 how to induce your gene of interest without inducing misinterpretations. Mol Biol Cell
683 32, 1517–1522. https://doi.org/10.1091/mbc.E21-04-0177
684 **Erler, A., Maresca, M., Fu, J., Stewart, A.F.** (2006). Recombineering reagents for
685 improved inducible expression and selection marker re-use in Schizosaccharomyces
686 pombe. Yeast 23, 813–823. https://doi.org/10.1002/yea.1396
687 **Faryar, K., Gatz, C.** (1992). Construction of a Tetracycline-inducible promoter in
688 Schizosaccharomyces pombe. Curr Genet 21, 345–349.
689 https://doi.org/10.1007/BF00351693
690 **Forsburg, S.L.** (1993). Comparison of Schizosaccharomyces pombe expression
691 systems. Nucleic Acids Res 21, 2955–2956. https://doi.org/10.1093/nar/21.12.2955
692 **Fujita, Y., Tohda, H., Giga-Hama, Y., Takegawa, K.** (2006). Heat shock-inducible
693 expression vectors for use in Schizosaccharomyces pombe. FEMS Yeast Res 6, 883–
694 887. https://doi.org/10.1111/j.1567-1364.2006.00093.x
695 **Garg, A.** (2020). A lncRNA-regulated gene expression system with rapid induction
696 kinetics in the fission yeast Schizosaccharomyces pombe. RNA 26, 1743–1752.
697 https://doi.org/10.1261/rna.076000.120

Garí, E., Piedrafita, L., Aldea, M., Herrero, E. (1997). A set of vectors with a tetracycline-regulatable promoter system for modulated gene expression in Saccharomyces cerevisiae. Yeast 13, 837–848. https://doi.org/10.1002/(SICI)1097-0061(199707)13:9<837::AID-YEA145>3.0.CO;2-T

Gossen, M., Bonin, A.L., Bujard, H. (1993). Control of gene activity in higher eukaryotic cells by prokaryotic regulatory elements. Trends Biochem Sci 18, 471–475. https://doi.org/10.1016/0968-0004(93)90009-c

Guerra-Moreno, A., Alves-Rodrigues, I., Hidalgo, E., Ayté, J. (2012). Chemical genetic induction of meiosis in Schizosaccharomyces pombe. Cell Cycle 11, 1621–1625. https://doi.org/10.4161/cc.20051

He, L., Binari, R., Huang, J., Falo-Sanjuan, J., Perrimon, N. (2019). In vivo study of gene expression with an enhanced dual-color fluorescent transcriptional timer. Elife 8, e46181. https://doi.org/10.7554/eLife.46181

Hennig, S., Hornauer, N., Rödel, G., Ostermann, K. (2018). Pheromone-inducible expression vectors for fission yeast Schizosaccharomyces pombe. Plasmid 95, 1–6. https://doi.org/10.1016/j.plasmid.2017.11.002

Hillen, W., Gatz, C., Altschmied, L., Schollmeier, K., Meier, I. (1983). Control of expression of the Tn10-encoded tetracycline resistance genes. Equilibrium and kinetic investigation of the regulatory reactions. J Mol Biol 169, 707–721. https://doi.org/10.1016/s0022-2836(83)80166-1

Hillen, W., Schollmeier, K., Gatz, C. (1984). Control of expression of the Tn10-encoded tetracycline resistance operon. II. Interaction of RNA polymerase and TET repressor with the tet operon regulatory region. J Mol Biol 172, 185–201. https://doi.org/10.1016/s0022-2836(84)80037-6

Hoffman, C.S., Winston, F. (1989). A transcriptionally regulated expression vector for the fission yeast Schizosaccharomyces pombe. Gene 84, 473–479. https://doi.org/10.1016/0378-1119(89)90523-4

Iacovoni, J.S., Russell, P., Gaits, F. (1999). A new inducible protein expression system in fission yeast based on the glucose-repressed inv1 promoter. Gene 232, 53–58. https://doi.org/10.1016/S0378-1119(99)00116-X

Iino, Y., Yamamoto, M. (1985). Negative control for the initiation of meiosis in Schizosaccharomyces pombe. Proc Natl Acad Sci U S A 82, 2447–2451. https://doi.org/10.1073/pnas.82.8.2447

Jacobs, J.Z., Ciccaglione, K.M., Tournier, V., Zaratiegui, M. (2014). Implementation of the CRISPR-Cas9 system in fission yeast. Nat Commun 5, 5344. https://doi.org/10.1038/ncomms6344

Kelly, M., Burke, J., Smith, M., Klar, A., Beach, D. (1988). Four mating-type genes

control sexual differentiation in the fission yeast. EMBO J 7, 1537–1547.
Kelly, T.J., Martin, G.S., Forsburg, S.L., Stephen, R.J., Russo, A., Nurse, P. (1993). The fission yeast cdc18+ gene product couples S phase to START and mitosis. Cell 74, 371–382. https://doi.org/10.1016/0092-8674(93)90427-r
Kjaerulff, S., Nielsen, O. (2015). An IPTG-inducible derivative of the fission yeast nmt promoter. Yeast 32, 469–478. https://doi.org/10.1002/yea.3073
Kumar, R., Singh, J. (2006). A truncated derivative of nmt 1 promoter exhibits temperature-dependent induction of gene expression in Schizosaccharomyces pombe. Yeast 23, 55–65. https://doi.org/10.1002/yea.1343
Lamping, E., Niimi, M., Cannon, R.D. (2013). Small, synthetic, GC-rich mRNA stem-loop modules 5' proximal to the AUG start-codon predictably tune gene expression in yeast. Microb Cell Fact 12, 74. https://doi.org/10.1186/1475-2859-12-74
Lemay, J.-F., Larochelle, M., Marguerat, S., Atkinson, S., Bähler, J., Bachand, F. (2014). The RNA exosome promotes transcription termination of backtracked RNA polymerase II. Nat Struct Mol Biol 21, 919–926. https://doi.org/10.1038/nsmb.2893
Li, H., Hou, J., Bai, L., Hu, C., Tong, P., Kang, Y., Zhao, X., Shao, Z. (2015). Genome-wide analysis of core promoter structures in Schizosaccharomyces pombe with DeepCAGE. RNA Biol 12, 525–537. https://doi.org/10.1080/15476286.2015.1022704
Li, R., Jin, M., Du, J., Li, M., Chen, S., Yang, S. (2020). The Magnesium Concentration in Yeast Extracts Is a Major Determinant Affecting Ethanol Fermentation Performance of Zymomonas mobilis. Front Bioeng Biotechnol 8, 957. https://doi.org/10.3389/fbioe.2020.00957
Lu, Z., Lin, Z. (2021). The origin and evolution of a distinct mechanism of transcription initiation in yeasts. Genome Res 31, 51–63. https://doi.org/10.1101/gr.264325.120
Madar, D., Dekel, E., Bren, A., Alon, U. (2011). Negative auto-regulation increases the input dynamic-range of the arabinose system of Escherichia coli. BMC Syst Biol 5, 111. https://doi.org/10.1186/1752-0509-5-111
Marguerat, S., Schmidt, A., Codlin, S., Chen, W., Aebersold, R., Bähler, J. (2012). Quantitative analysis of fission yeast transcriptomes and proteomes in proliferating and quiescent cells. Cell 151, 671–683. https://doi.org/10.1016/j.cell.2012.09.019
Matsuzawa, T., Tohda, H., Takegawa, K. (2013). Ethanol-inducible gene expression using gld1 (+) promoter in the fission yeast Schizosaccharomyces pombe. Appl Microbiol Biotechnol 97, 6835–6843. https://doi.org/10.1007/s00253-013-4812-2
Matynia, A., Salus, S.S., Sazer, S. (2002). Three proteins required for early steps in the protein secretory pathway also affect nuclear envelope structure and cell cycle progression in fission yeast. J Cell Sci 115, 421–431.

https://doi.org/10.1242/jcs.115.2.421
Maundrell, K. (1993). Thiamine-repressible expression vectors pREP and pRIP for fission yeast. Gene 123, 127–130. https://doi.org/10.1016/0378-1119(93)90551-d
Maundrell, K. (1990). nmt1 of fission yeast. A highly transcribed gene completely repressed by thiamine. Journal of Biological Chemistry 265, 10857–10864. https://doi.org/10.1016/S0021-9258(19)38525-4
Moreno, M.B., Durán, A., Ribas, J.C. (2000). A family of multifunctional thiamine-repressible expression vectors for fission yeast. Yeast 16, 861–872. https://doi.org/10.1002/1097-0061(20000630)16:9<861::AID-YEA577>3.0.CO;2-9
Moullan, N., Mouchiroud, L., Wang, X., Ryu, D., Williams, E.G., Mottis, A., Jovaisaite, V., Frochaux, M.V., Quiros, P.M., Deplancke, B. et al. (2015). Tetracyclines Disturb Mitochondrial Function across Eukaryotic Models: A Call for Caution in Biomedical Research. Cell Rep 10, 1681–1691. https://doi.org/10.1016/j.celrep.2015.02.034
Murphy, K.F., Balázsi, G., Collins, J.J. (2007). Combinatorial promoter design for engineering noisy gene expression. Proc Natl Acad Sci U S A 104, 12726–12731. https://doi.org/10.1073/pnas.0608451104
Nevozhay, D., Adams, R.M., Murphy, K.F., Josic, K., Balázsi, G. (2009). Negative autoregulation linearizes the dose-response and suppresses the heterogeneity of gene expression. Proc Natl Acad Sci U S A 106, 5123–5128. https://doi.org/10.1073/pnas.0809901106
Newville, M., Stensitzki, T., Allen, D.B., Rawlik, M., Ingargiola, A., Nelson, A. (2016). Lmfit: Non-Linear Least-Square Minimization and Curve-Fitting for Python. Astrophysics Source Code Library ascl:1606.014.
Ohira, M.J., Hendrickson, D.G., Scott McIsaac, R., Rhind, N. (2017). An estradiol-inducible promoter enables fast, graduated control of gene expression in fission yeast. Yeast 34, 323–334. https://doi.org/10.1002/yea.3235
Ottilie, S., Miller, P.J., Johnson, D.I., Creasy, C.L., Sells, M.A., Bagrodia, S., Forsburg, S.L., Chernoff, J. (1995). Fission yeast pak1+ encodes a protein kinase that interacts with Cdc42p and is involved in the control of cell polarity and mating. EMBO J 14, 5908–5919. https://doi.org/10.1002/j.1460-2075.1995.tb00278.x
Patterson, J.O., Rees, P., Nurse, P. (2019). Noisy Cell-Size-Correlated Expression of Cyclin B Drives Probabilistic Cell-Size Homeostasis in Fission Yeast. Current Biology 29, 1379-1386.e4. https://doi.org/10.1016/j.cub.2019.03.011
Perruca-Foncillas, R., Davidsson, J., Carlquist, M., Gorwa-Grauslund, M.F. (2022). Assessment of fluorescent protein candidates for multi-color flow cytometry analysis of Saccharomyces cerevisiae. Biotechnol Rep (Amst) 34, e00735.

https://doi.org/10.1016/j.btre.2022.e00735
Petersen, J., Hagan, I.M. (2003). S. pombe aurora kinase/survivin is required for chromosome condensation and the spindle checkpoint attachment response. Curr Biol 13, 590–597. https://doi.org/10.1016/s0960-9822(03)00205-7
Petersen, J., Russell, P. (2016). Growth and the Environment of Schizosaccharomyces pombe. Cold Spring Harb Protoc 2016, pdb.top079764. https://doi.org/10.1101/pdb.top079764
Picard, D., Schena, M., Yamamoto, K.R. (1990). An inducible expression vector for both fission and budding yeast. Gene 86, 257–261. https://doi.org/10.1016/0378-1119(90)90287-2
Politi, N., Pasotti, L., Zucca, S., Casanova, M., Micoli, G., Cusella De Angelis, M.G., Magni, P. (2014). Half-life measurements of chemical inducers for recombinant gene expression. J Biol Eng 8, 5. https://doi.org/10.1186/1754-1611-8-5
Rasmussen, B., Noller, H.F., Daubresse, G., Oliva, B., Misulovin, Z., Rothstein, D.M., Ellestad, G.A., Gluzman, Y., Tally, F.P., Chopra, I. (1991). Molecular basis of tetracycline action: identification of analogs whose primary target is not the bacterial ribosome. Antimicrob Agents Chemother 35, 2306–2311. https://doi.org/10.1128/AAC.35.11.2306
Rosenfeld, N., Elowitz, M.B., Alon, U. (2002). Negative autoregulation speeds the response times of transcription networks. J Mol Biol 323, 785–793. https://doi.org/10.1016/s0022-2836(02)00994-4
Russell, P.R. (1983). Evolutionary divergence of the mRNA transcription initiation mechanism in yeast. Nature 301, 167–169. https://doi.org/10.1038/301167a0
Rutherford, K.M., Lera-Ramírez, M., Wood, V. (2024). PomBase: a Global Core Biodata Resource-growth, collaboration, and sustainability. Genetics 227, iyae007. https://doi.org/10.1093/genetics/iyae007
Schindelin, J., Arganda-Carreras, I., Frise, E., Kaynig, V., Longair, M., Pietzsch, T., Preibisch, S., Rueden, C., Saalfeld, S., Schmid, B. et al. (2012). Fiji: an open-source platform for biological-image analysis. Nat Methods 9, 676–682. https://doi.org/10.1038/nmeth.2019
Shiroiwa, Y., Hayashi, T., Fujita, Y., Villar-Briones, A., Ikai, N., Takeda, K., Ebe, M., Yanagida, M. (2011). Mis17 is a regulatory module of the Mis6-Mal2-Sim4 centromere complex that is required for the recruitment of CenH3/CENP-A in fission yeast. PLoS One 6, e17761. https://doi.org/10.1371/journal.pone.0017761
Smith, G.R. (2009). Genetic Analysis of Meiotic Recombination in Schizosaccharomyces pombe. Methods Mol Biol 557, 65–76.
Stringer, C., Wang, T., Michaelos, M., Pachitariu, M. (2021). Cellpose: a generalist

algorithm for cellular segmentation. Nat Methods 18, 100–106. https://doi.org/10.1038/s41592-020-01018-x

Sunder, S., Greeson-Lott, N.T., Runge, K.W., Sanders, S.L. (2012). A new method to efficiently induce a site-specific double-strand break in the fission yeast Schizosaccharomyces pombe. Yeast 29, 275–291. https://doi.org/10.1002/yea.2908

Tajadura, V., García, B., García, I., García, P., Sánchez, Y. (2004). Schizosaccharomyces pombe Rgf3p is a specific Rho1 GEF that regulates cell wall beta-glucan biosynthesis through the GTPase Rho1p. J Cell Sci 117, 6163–6174. https://doi.org/10.1242/jcs.01530

Thodberg, M., Thieffry, A., Bornholdt, J., Boyd, M., Holmberg, C., Azad, A., Workman, C.T., Chen, Y., Ekwall, K., Nielsen, O. et al. (2019). Comprehensive profiling of the fission yeast transcription start site activity during stress and media response. Nucleic Acids Res 47, 1671–1691. https://doi.org/10.1093/nar/gky1227

Tommasino, M., Maundrell, K. (1991). Uptake of thiamine by Schizosaccharomyces pombe and its effect as a transcriptional regulator of thiamine-sensitive genes. Curr Genet 20, 63–66. https://doi.org/10.1007/BF00312766

Torres-Garcia, S., Yaseen, I., Shukla, M., Audergon, P.N.C.B., White, S.A., Pidoux, A.L., Allshire, R.C. (2020). Epigenetic gene silencing by heterochromatin primes fungal resistance. Nature 585, 453–458. https://doi.org/10.1038/s41586-020-2706-x

Toyama, R., Okayama, H. (1990). Human chorionic gonadotropin alpha and human cytomegalovirus promoters are extremely active in the fission yeast Schizosaccharomyces pombe. FEBS Lett 268, 217–221. https://doi.org/10.1016/0014-5793(90)81012-d

Vještica, A., Marek, M., Nkosi, P.J., Merlini, L., Liu, G., Bérard, M., Billault-Chaumartin, I., Martin, S.G. (2020). A toolbox of stable integration vectors in the fission yeast Schizosaccharomyces pombe. Journal of Cell Science 133, jcs240754. https://doi.org/10.1242/jcs.240754

Waisman, A., Norris, A.M., Elías Costa, M., Kopinke, D. (2021). Automatic and unbiased segmentation and quantification of myofibers in skeletal muscle. Sci Rep 11, 11793. https://doi.org/10.1038/s41598-021-91191-6

Wang, H., Tang, X., Liu, J., Trautmann, S., Balasundaram, D., McCollum, D., Balasubramanian, M.K. (2002). The multiprotein exocyst complex is essential for cell separation in Schizosaccharomyces pombe. Mol Biol Cell 13, 515–529. https://doi.org/10.1091/mbc.01-11-0542

Wang, Hongcheng, Wang, Haiyang, Wang, M., Zhang, L., Wang, R., Mei, Y., Shao, W. (2014). Identification and refinement of two strong constitutive promoters for

883 gene expression system of Schizosaccharomyces pombe. World J Microbiol Biotechnol
884 30, 1809–1817. https://doi.org/10.1007/s11274-014-1603-6
885 **Wang, J., Eisenstatt, J.R., Audry, J., Cornelius, K., Shaughnessy, M., Berkner,**
886 **K.L., Runge, K.W.** (2018). A Heterochromatin Domain Forms Gradually at a New
887 Telomere and Is Dynamic at Stable Telomeres. Mol Cell Biol 38, e00393-17.
888 https://doi.org/10.1128/MCB.00393-17
889 **Watson, A.T., Werler, P., Carr, A.M.** (2011). Regulation of gene expression at the
890 fission yeast Schizosaccharomyces pombe urg1 locus. Gene 484, 75–85.
891 https://doi.org/10.1016/j.gene.2011.05.028
892 **Watt, S., Mata, J., López-Maury, L., Marguerat, S., Burns, G., Bähler, J.** (2008).
893 urg1: A Uracil-Regulatable Promoter System for Fission Yeast with Short Induction
894 and Repression Times. PLOS ONE 3, e1428.
895 https://doi.org/10.1371/journal.pone.0001428
896 **Westwood, P.K., Martin, I.V., Fantes, P.A.** (2004). Fission yeast Cdc37 is required
897 for multiple cell cycle functions. Mol Genet Genomics 271, 82–90.
898 https://doi.org/10.1007/s00438-003-0958-4
899 **Win, T.Z., Goodwin, A., Hickson, I.D., Norbury, C.J., Wang, S.-W.** (2004).
900 Requirement for Schizosaccharomyces pombe Top3 in the maintenance of chromosome
901 integrity. J Cell Sci 117, 4769–4778. https://doi.org/10.1242/jcs.01351
902 **Wray, L.V., Reznikoff, W.S.** (1983). Identification of repressor binding sites
903 controlling expression of tetracycline resistance encoded by Tn10. J Bacteriol 156,
904 1188–1191. https://doi.org/10.1128/jb.156.3.1188-1191.1983
905 **Yamamoto, A., Hiraoka, Y.** (2003). Monopolar spindle attachment of sister
906 chromatids is ensured by two distinct mechanisms at the first meiotic division in fission
907 yeast. The EMBO Journal 22, 2284–2296. https://doi.org/10.1093/emboj/cdg222
908 **Yue, M., Zeng, L., Singh, A., Xu, Y.** (2014). Rad4 mainly functions in Chk1-mediated
909 DNA damage checkpoint pathway as a scaffold protein in the fission yeast
910 Schizosaccharomyces pombe. PLoS One 9, e92936.
911 https://doi.org/10.1371/journal.pone.0092936
912 **Zhang, X.-R., He, J.-B., Wang, Y.-Z., Du, L.-L.** (2018). A Cloning-Free Method for
913 CRISPR/Cas9-Mediated Genome Editing in Fission Yeast. G3 (Bethesda) 8, 2067–
914 2077. https://doi.org/10.1534/g3.118.200164
915 **Zhang, X.-R., Zhao, L., Suo, F., Gao, Y., Wu, Q., Qi, X., Du, L.-L.** (2022). An
916 improved auxin-inducible degron system for fission yeast. G3 Genes|Genomes|Genetics
917 12, jkab393. https://doi.org/10.1093/g3journal/jkab393
918 **Zhang, Y., Boyd, S.A., Teppen, B.J., Tiedje, J.M., Li, H.** (2014). Role of tetracycline
919 speciation in the bioavailability to Escherichia coli for uptake and expression of

920 antibiotic resistance. Environ Sci Technol 48, 4893–4900.
921 https://doi.org/10.1021/es5003428
922 **Zilio, N., Wehrkamp-Richter, S., Boddy, M.N.** (2012). A new versatile system for
923 rapid control of gene expression in the fission yeast Schizosaccharomyces pombe. Yeast
924 29, 425–434. https://doi.org/10.1002/yea.2920
925
926

927 **Figure legends**

928 **Fig. 1. Overview of the new tetracycline-inducible expression system.**

929 (A) Schematic showing how the *enotetS* promoter (*PenotetS*) was generated. *PenotetS* was
930 engineered from the *eno101* promoter (*Peno101*) by introducing a single 19-bp *tetO*
931 sequence between the TATA box and the transcription start site (TSS) of *Peno101*, while
932 maintaining the original distance between the TATA box and the TSS.

933 (B) Diagram of the integration plasmid pDB5318. This plasmid contains *PenotetS* and a
934 TetR-expressing cassette, which consists of the cytomegalovirus promoter (*P.CMV*) and
935 the TetR coding sequence. The plasmid can be integrated at the *ade6* locus following
936 linearization with NotI digestion. The mECitrine coding sequence can be replaced with
937 the sequence of any desired gene to be expressed under the control of *PenotetS*, using
938 the NheI and BglII restriction sites.

939 (C) Schematic of four weakened variants of *PenotetS*. These variants were created by
940 inserting a GC-rich stem-loop-forming sequence downstream of *PenotetS*. Bases
941 forming the stem are highlighted in red, while those forming the loop are shown in black.

942 (D) Fluorescence of cells expressing the yellow fluorescent protein mECitrine from each of
943 the *enotetS* series promoters and from the *adh1* promoter in the presence and absence
944 of the inducer anhydrotetracycline (ahTet). Cells were imaged after 24 hours of growth in
945 YES medium in the presence of ahTet or DMSO (solvent control). The images are
946 presented with two different display ranges to enhance the visualization of differences in
947 fluorescence intensities. Scale bar, 10 μm.

948

949 **Fig. 2. Inducer dose response of *PenotetS*.**

950 (A) Inducer dose response in YES medium. Cells expressing mECitrine from *PenotetS* were
951 grown in YES medium in the presence of different doses of the inducer ahTet and then
952 imaged. Scale bar, 10 μm.

953 (B) Quantification of mECitrine fluorescence in the imaging data from the experiment shown
954 in A. The fluorescence level in the presence of 2.5 μg/ml ahTet was used as a reference
955 for normalization (100% expression level).

956 (C) Inducer dose response in EMM medium. Cells expressing mECitrine from *PenotetS* were
957 grown in EMM medium in the presence of different doses of the inducer ahTet and then
958 imaged. Scale bar, 10 μm.

959 (D) Quantification of mECitrine fluorescence in the imaging data from the experiment shown
960 in C. The fluorescence level in the presence of 2.5 μg/ml ahTet was used as a reference
961 for normalization (100% expression level).

962

963 **Fig. 3. Induction kinetics of *PenotetS* and *PenotetSW2* in dividing cells.**

964 (A) Time-course analysis of the induction kinetics of *PenotetS* in log-phase cells grown in
965 YES and EMM media. Images of cells expressing mECitrine from *PenotetS* were taken
966 at the indicated time points after the addition of 2.5 μg/ml ahTet to the culture. Scale bar,
967 10 μm.

968 (B, C) Quantification of mECitrine fluorescence in the imaging data from the experiment
969 shown in A. The fluorescence level at the 24-hour time point was used as a reference for
970 normalization (100% expression level). The curves depict the mathematical model of the
971 induction kinetics, with the modeled half-life value presented beneath each curve.

972 (D, E) Induction kinetics of *PenotetSW2* in log-phase cells grown in YES and EMM media.
973 Data processing and presentation were carried out as described in (B, C).

974

975 **Fig. 4. Expression levels of different promoters.**

976 (A) Expression levels in YES medium. Cells expressing mECitrine from *Padh1* and from
977 each of the *enotetS* series promoters were grown in YES medium under induced
978 conditions (abbreviated as ind., in the presence of ahTet) and repressed conditions
979 (abbreviated as rep., in the absence of ahTet), and then imaged. The quantification
980 results from two biological replicates and their mean values are shown. A thick dashed
981 line represents a threshold (THR) below which the mECitrine fluorescence level cannot
982 be accurately determined. This threshold corresponds to 2% of the average background
983 fluorescence in a parental strain lacking mECitrine.

984 (B) Expression levels in EMM medium. Cells expressing mECitrine from each of the *enotetS*
985 series promoters were grown in EMM medium under induced conditions (in the presence
986 of ahTet) and repressed conditions (in the absence of ahTet), and then imaged. Cells
987 expressing mECitrine from each of the *nmt1* series promoters were grown in EMM
988 medium under induced conditions (in the absence of thiamine) and repressed conditions
989 (in the presence of thiamine), and then imaged. The images are presented with two
990 different display ranges to enhance the visualization of differences in fluorescence
991 intensities. Scale bar, 10 μm.

992 (C) Quantification of mECitrine fluorescence in the imaging data from the experiment shown
993 in B. The quantification results from two biological replicates and their mean values are
994 shown.

995 (D) The induced expression level based on the mECitrine fluorescence (normalized to that
996 of *Pnmt1*) and the estimated number of mRNA molecules per cell based on the reported
997 value of 340 for the number of mRNA molecules per cell for the *nmt1* gene.

998

999 **Fig. 5. Induction kinetics of *PenotetS* in quiescent cells.**

1000 (A) Time-course analysis of the induction kinetics of *PenotetS* in G0 cells in EMM−N medium.
1001 Images were taken at the indicated time points after the addition of 2.5 μg/ml ahTet. Scale
1002 bar, 10 μm.

1003 (B) Time-course analysis of the induction kinetics of *PenotetS* in spores in EMM−N medium.
1004 Images were taken at the indicated time points after the addition of 2.5 μg/ml ahTet. Scale
1005 bar, 10 μm.

1006 (C) Quantification of mECitrine fluorescence in the imaging data from the experiments shown
1007 in A and B, as well as a control experiment in which log-phase cells were grown in EMM
1008 medium. Three biological replicates were conducted, and one representative dataset is
1009 shown here. The graph on the left uses a linear scale for the y-axis, while the graph on
1010 the right uses a logarithmic scale. The curves depict the mathematical model of the
1011 induction kinetics, with the modeled half-life values presented in the graph on the right.

1012

1013 **Fig. 6. A new method for synchronous meiosis induction based on the expression of**
1014 ***Mc-2A-Mi* from *PenotetSW1* in *h+/h+* diploids.**
1015 (A) Schematic illustrating the new method for synchronous meiosis induction.
1016 (B) Progression of meiosis monitored by DNA staining. Cell samples were stained with the
1017 DNA dye SYTOX Green and imaged at the indicated time points after the addition of
1018 ahTet. Manual counting was performed to determine the percentages of cells containing
1019 different numbers of nuclei. Three biological replicates were conducted, and one
1020 representative dataset is shown here.
1021 (C) Viability of spores from induced meiosis. Tetrad analysis was performed on YES plates.
1022

1023 **Fig. 7. Generation of conditional loss-of-function mutants using the *enotetS* series**
1024 **promoters.**
1025 (A) Tetrad analysis of heterozygous deletion diploids carrying an integration plasmid
1026 expressing the deleted gene from either *PenotetSW2* or *PenotetSW3*. Diploids were
1027 sporulated, and the resulting tetrads were dissected on YES plates with and without
1028 ahTet. Four spores from a single ascus are labeled A, B, C, and D. The genotype of
1029 inviable spores was inferred based on the assumption of 2:2 segregation. Induced
1030 expression of *sui1* and *nrs1* rescued the lethality of the respective deletions, while
1031 repressed expression did not.
1032 (B) Growth curve analysis showing that the growth defect caused by shutting off gene
1033 expression through the removal of ahTet arises rapidly. Cells were initially cultured for
1034 24 hours in YES liquid medium containing ahTet. Following this, cells were washed
1035 three times with water and transferred to both ahTet-containing and ahTet-free YES
1036 media. The optical density at 600 nm (OD600) of each culture was measured at the
1037 indicated time points. Cultures were diluted when the OD600 approached 1.0 to
1038 maintain logarithmic growth. The number of generations was calculated based on the
1039 OD600 measurements and the dilution ratio.
1040

1041 **Fig. 8. Schematics depicting the improved tetracycline-inducible expression system**
1042 **developed in this study.**
1043 (A) Schematic illustrating the repressed and induced states of the *enotetS* promoter. In the
1044 absence of the inducer ahTet, TetR binds to *tetO*, repressing the transcription of the
1045 downstream gene. Upon the addition of ahTet, the ahTet-bound TetR undergoes a
1046 conformational change, preventing it from binding to *tetO* and thereby allowing the
1047 transcription of the downstream gene to be induced. The induced state can be reverted
1048 back to the repressed state by removing ahTet.
1049 (B) Schematic illustrating the five distinct expression levels of the *enotetS* series promoters.
1050 Four different stem-loop-forming sequences were individually inserted immediately
1051 downstream of *PenotetS*, resulting in four weakened variants: *PenotetSW1*, *PenotetSW2*,
1052 *PenotetSW3*, and *PenotetSW4*. The degree of expression attenuation increases with the
1053 number of GC base pairs in the stem.
1054

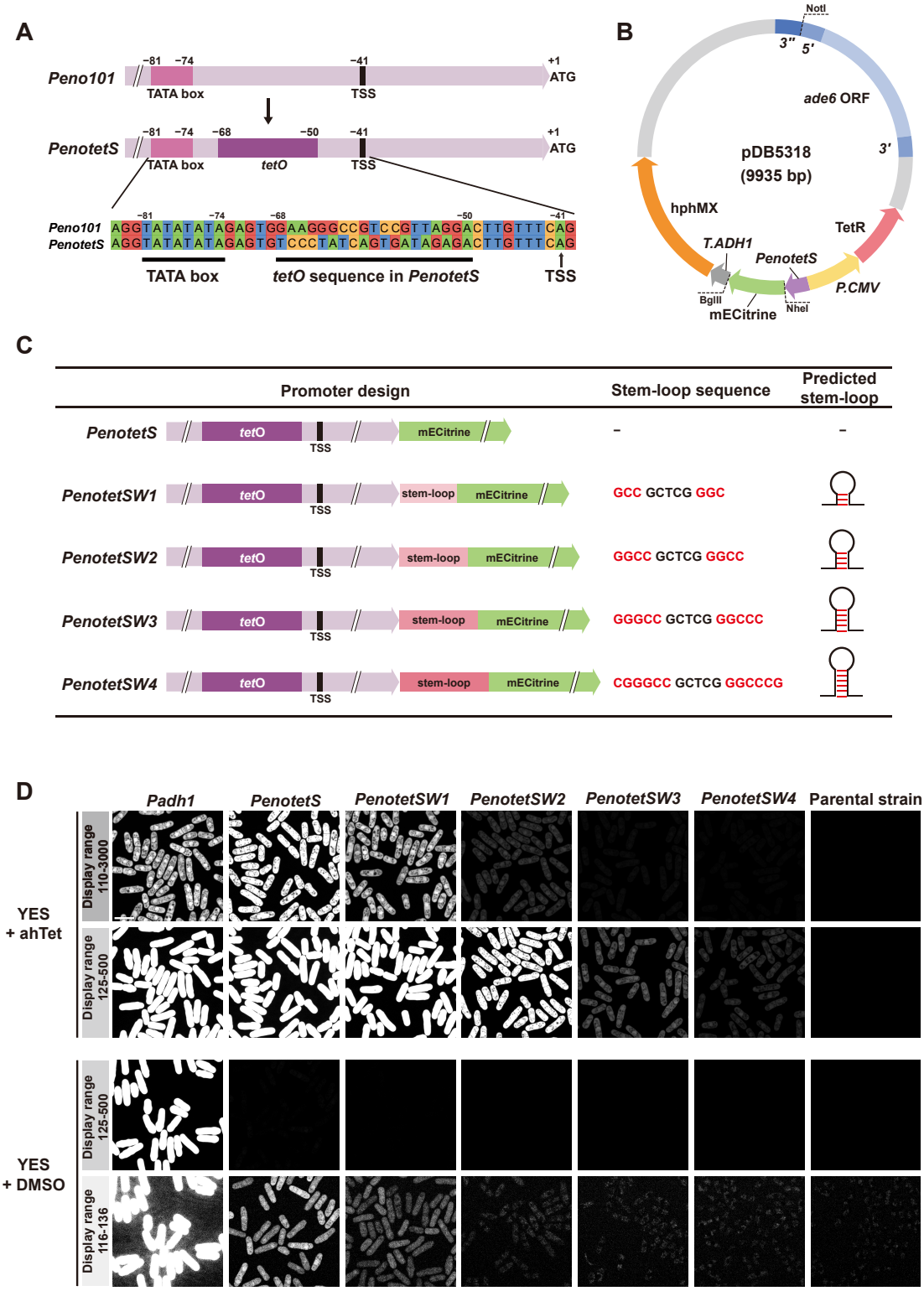
A
Peno101
−81
−74
−41
+1
ATG
TATA box
TSS
PenotetS
−68
−50
tetO
Peno101 AGGTATATATAGAGTGGAAGGGCCGTCCGTTAGGACTTGTTTCAG
PenotetS AGGTATATATAGAGTGTCCCTATCAGTGATAGAGACTTGTTTCAG
TATA box
tetO sequence in PenotetS
TSS
B
NotI
3''
5'
ade6 ORF
3'
pDB5318
(9935 bp)
hphMX
TetR
T.ADH1
PenotetS
P.CMV
BglII
NheI
mECitrine
C
Promoter design
Stem-loop sequence
Predicted stem-loop
PenotetS
tetO
TSS
mECitrine
-
-
PenotetSW1
stem-loop
GCC GCTCG GGC
PenotetSW2
GGCC GCTCG GGCC
PenotetSW3
GGGCC GCTCG GGCCC
PenotetSW4
CGGGCC GCTCG GGCCCG
D
Padh1
PenotetS
PenotetSW1
PenotetSW2
PenotetSW3
PenotetSW4
Parental strain
YES
+ ahTet
Display range 110-3000
Display range 125-500
YES
+ DMSO
Display range 125-500
Display range 116-136

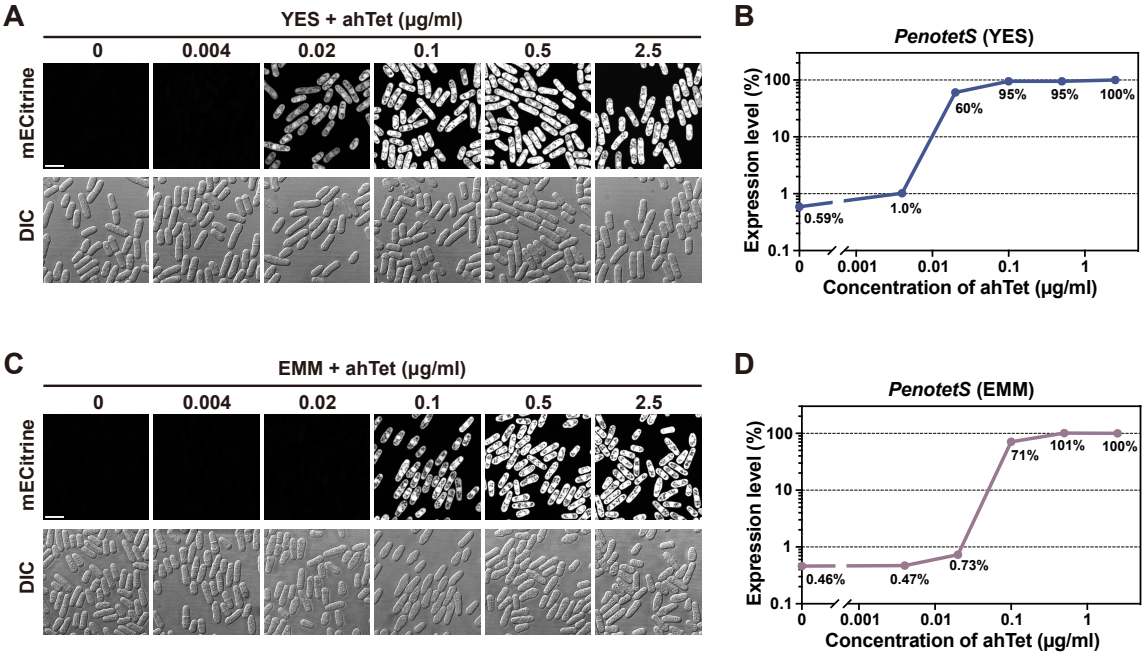
A
YES + ahTet (μg/ml)
0
0.004
0.02
0.1
0.5
2.5
mECitrine
DIC
B
PenotetS (YES)
Expression level (%)
100
10
1
0.1
0.59%
1.0%
60%
95%
95%
100%
0
0.001
0.01
0.1
1
Concentration of ahTet (μg/ml)
C
EMM + ahTet (μg/ml)
0
0.004
0.02
0.1
0.5
2.5
mECitrine
DIC
D
PenotetS (EMM)
Expression level (%)
100
10
1
0.1
0.46%
0.47%
0.73%
71%
101%
100%
0
0.001
0.01
0.1
1
Concentration of ahTet (μg/ml)

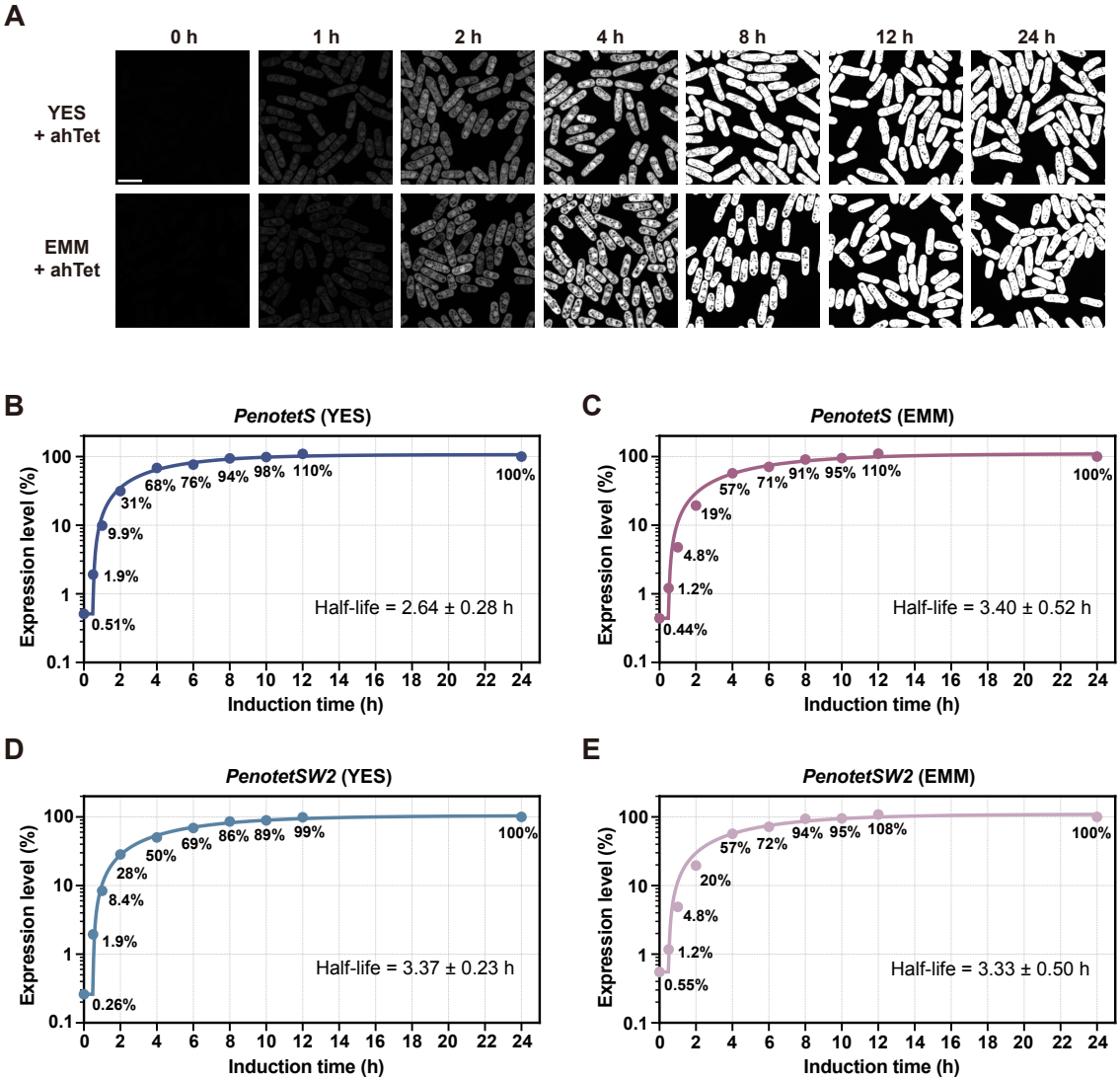
A
0 h
1 h
2 h
4 h
8 h
12 h
24 h
YES
+ ahTet
EMM
+ ahTet
B
PenotetS (YES)
Expression level (%)
Induction time (h)
0.51%
1.9%
9.9%
31%
68%
76%
94%
98%
110%
100%
Half-life = 2.64 ± 0.28 h
C
PenotetS (EMM)
0.44%
1.2%
4.8%
19%
57%
71%
91%
95%
110%
100%
Half-life = 3.40 ± 0.52 h
D
PenotetSW2 (YES)
0.26%
1.9%
8.4%
28%
50%
69%
86%
89%
99%
100%
Half-life = 3.37 ± 0.23 h
E
PenotetSW2 (EMM)
0.55%
1.2%
4.8%
20%
57%
72%
94%
95%
108%
100%
Half-life = 3.33 ± 0.50 h

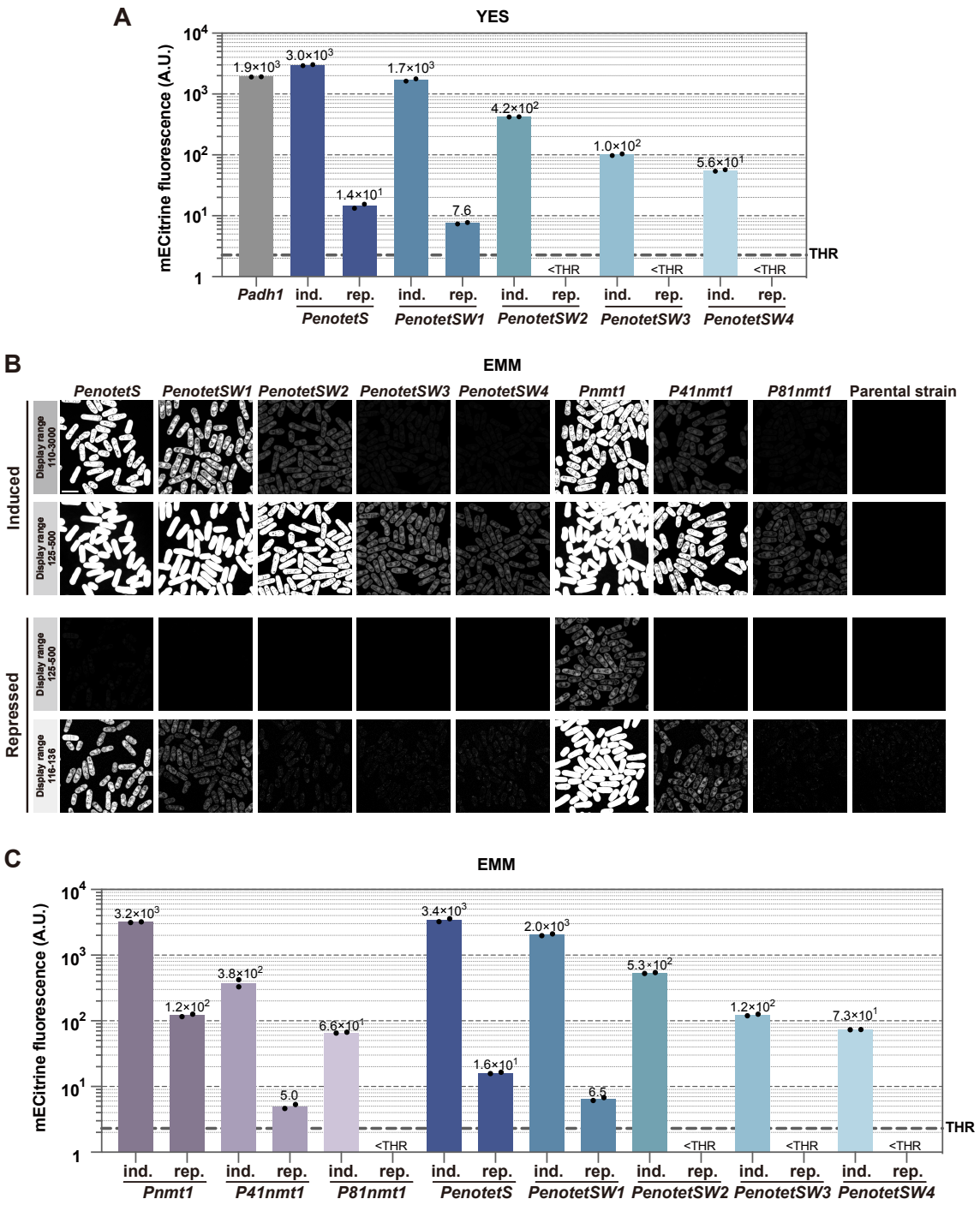

D

	Pnmt1	*PenotetS*	*PenotetSW1*	*PenotetSW2*	*PenotetSW3*	*PenotetSW4*
Induced expression level	1	1.073	0.643	0.168	0.039	0.023
Estimated mRNA level	340	365	219	57	13	8

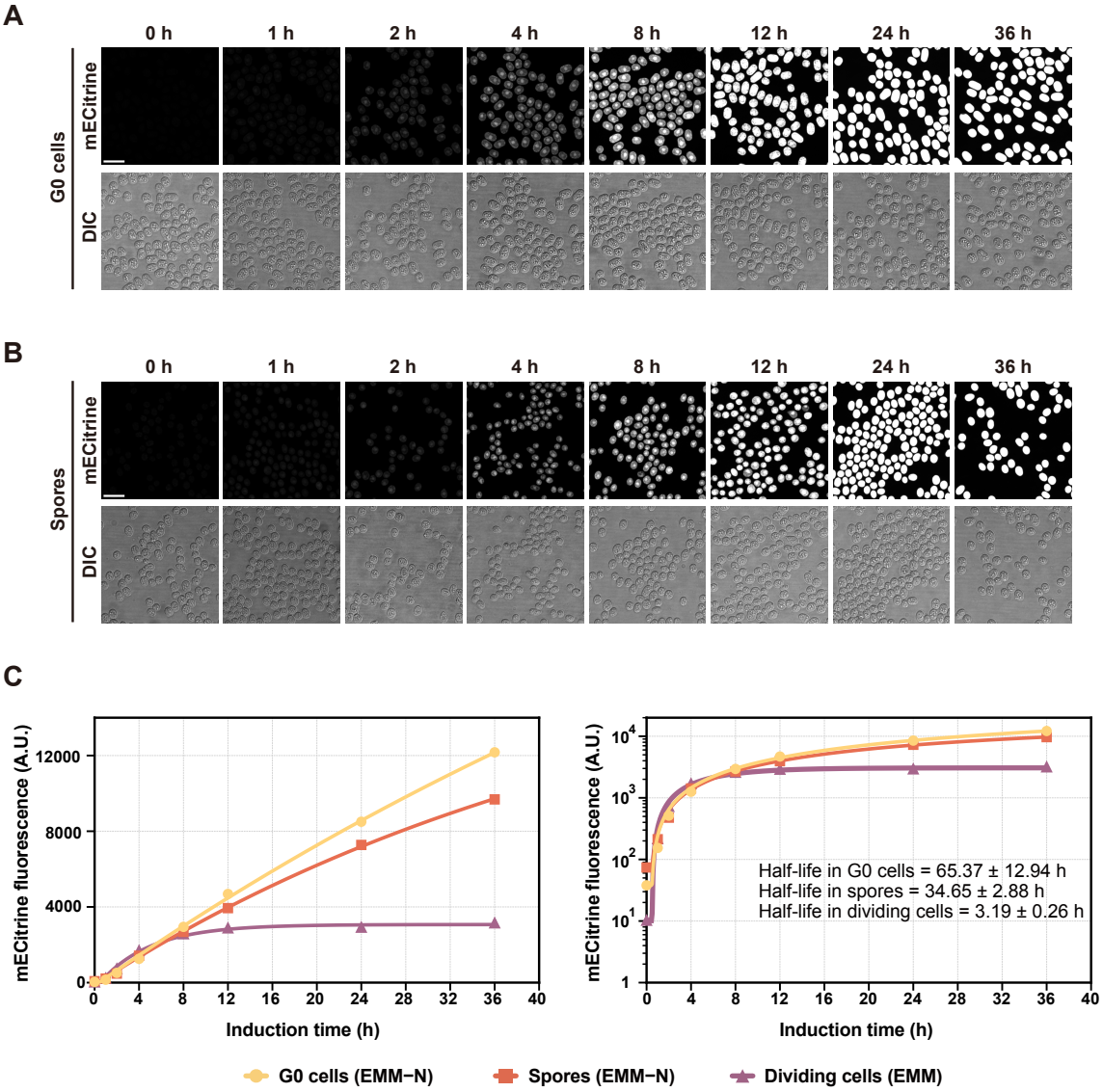
A
0 h
1 h
2 h
4 h
8 h
12 h
24 h
36 h
G0 cells
mECitrine
DIC
B
Spores
C
mECitrine fluorescence (A.U.)
Induction time (h)
Half-life in G0 cells = 65.37 ± 12.94 h
Half-life in spores = 34.65 ± 2.88 h
Half-life in dividing cells = 3.19 ± 0.26 h
G0 cells (EMM−N)
Spores (EMM−N)
Dividing cells (EMM)

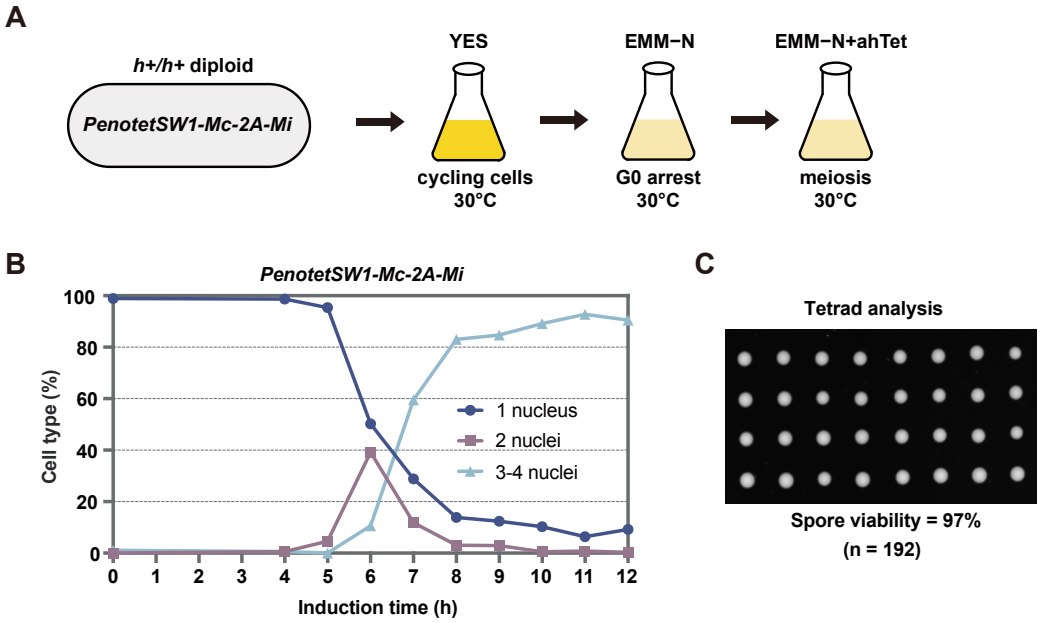
A
h+/h+ diploid
PenotetSW1-Mc-2A-Mi
YES
cycling cells
30°C
EMM−N
G0 arrest
30°C
EMM−N+ahTet
meiosis
30°C
B
PenotetSW1-Mc-2A-Mi
Cell type (%)
100
80
60
40
20
0
0 1 2 3 4 5 6 7 8 9 10 11 12
Induction time (h)
1 nucleus
2 nuclei
3-4 nuclei
C
Tetrad analysis
Spore viability = 97%
(n = 192)

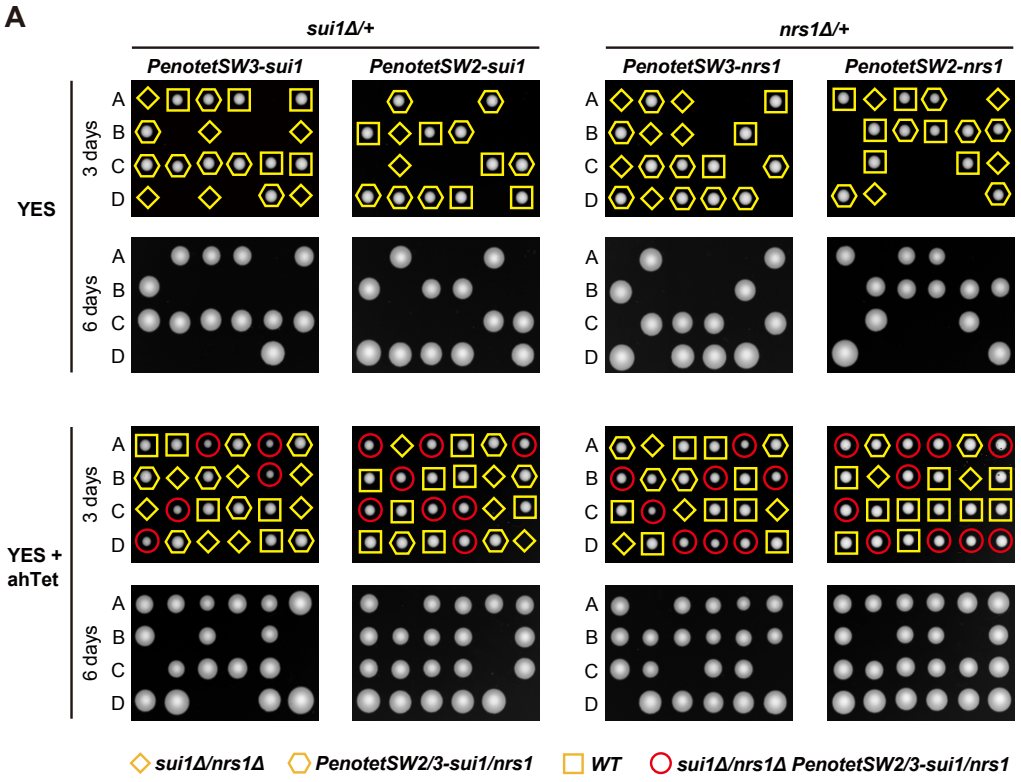
A
sui1Δ/+
nrs1Δ/+
PenotetSW3-sui1
PenotetSW2-sui1
PenotetSW3-nrs1
PenotetSW2-nrs1
YES
YES + ahTet
3 days
6 days
A
B
C
D
sui1Δ/nrs1Δ
PenotetSW2/3-sui1/nrs1
WT
sui1Δ/nrs1Δ PenotetSW2/3-sui1/nrs1

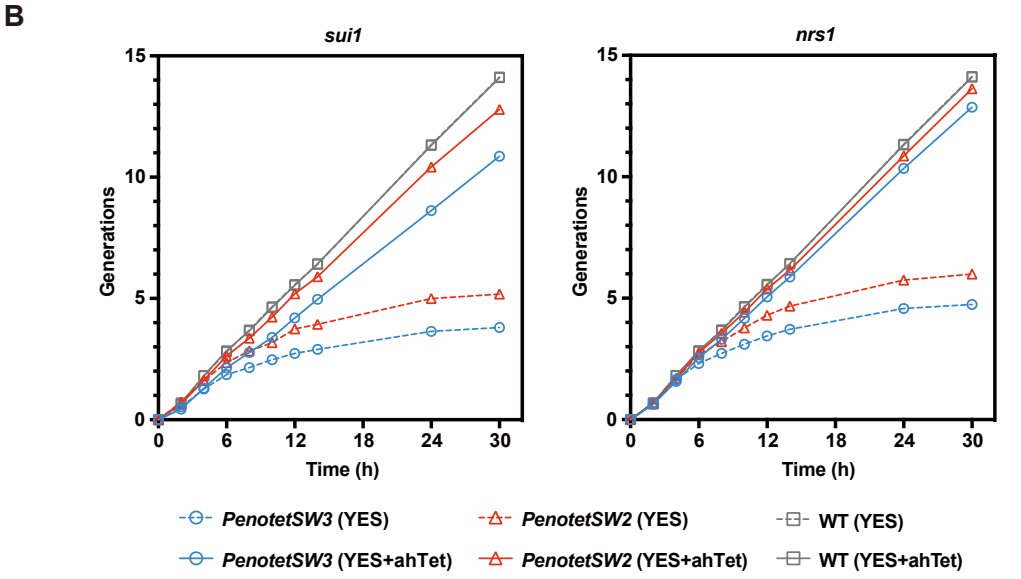
B
sui1
nrs1
Generations
Time (h)
0
5
10
15
0
6
12
18
24
30
PenotetSW3 (YES)
PenotetSW2 (YES)
WT (YES)
PenotetSW3 (YES+ahTet)
PenotetSW2 (YES+ahTet)
WT (YES+ahTet)

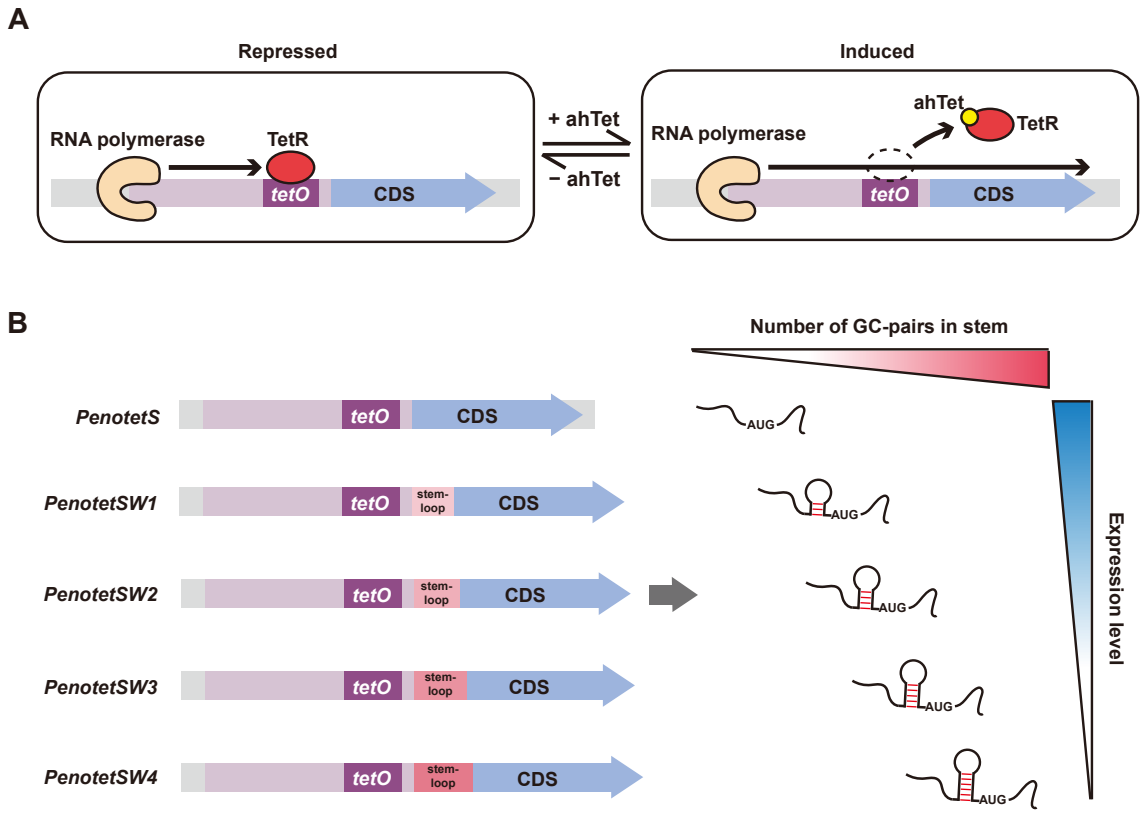
A
Repressed
Induced
RNA polymerase
TetR
tetO
CDS
+ ahTet
− ahTet
ahTet
B
Number of GC-pairs in stem
PenotetS
PenotetSW1
PenotetSW2
PenotetSW3
PenotetSW4
stem-loop
AUG
Expression level